AFRL-RX-TY-TP-2012-0062

DETERMINING THE INFECTIOUS DOSE OF INFLUENZA AEROSOLS IN A MOUSE MODEL

Rashelle S. McDonald

Student at the University of Saint Joseph—Connecticut
1678 Asylum Avenue
West Hartford, CT 06117-2791

July 2012

AIR FORCE RESEARCH LABORATORY
MATERIALS AND MANUFACTURING DIRECTORATE

■ **Air Force Materiel Command** ■ **United States Air Force** ■ **Tyndall Air Force Base, FL 32403-5323**

NOTICE AND SIGNATURE PAGE

WANDER.JOSEP
H.D.1230231660

Digitally signed by WANDER.JOSEPH.D.1230231660
DN: c=US, o=U.S. Government, ou=DoD, ou=PKI, ou=USAF, cn=WANDER.JOSEPH.D.1230231660
Date: 2012.07.13 15:24:36 -05'00'

JOSEPH D. WANDER, PhD
Work Unit Manager

HENLEY.MICHAE
L.V.1231823332

Digitally signed by HENLEY.MICHAEL.V.1231823332
DN: c=US, o=U.S. Government, ou=DoD, ou=PKI, ou=USAF, cn=HENLEY.MICHAEL.V.1231823332
Date: 2012.07.19 16:40:16 -05'00'

MICHAEL V. HENLEY, DR-IV
Program Manager

PILSON.DONNA.L
.1186939324

Digitally signed by PILSON.DONNA.L.1186939324
DN: c=US, o=U.S. Government, ou=DoD, ou=PKI, ou=USAF, cn=PILSON.DONNA.L.1186939324
Date: 2013.01.18 10:10:14 -06'00'

DONNA L. PILSON, LtCol, USAF
Deputy Chief, Airbase Technologies Division

REPORT DOCUMENTATION PAGE		Form Approved OMB No. 0704-0188

The public reporting burden for this collection of information is estimated to average 1 hour per response, including the time for reviewing instructions, searching existing data sources, gathering and maintaining the data needed, and completing and reviewing the collection of information. Send comments regarding this burden estimate or any other aspect of this collection of information, including suggestions for reducing the burden, to Department of Defense, Washington Headquarters Services, Directorate for Information Operations and Reports (0704-0188), 1215 Jefferson Davis Highway, Suite 1204, Arlington, VA 22202-4302. Respondents should be aware that notwithstanding any other provision of law, no person shall be subject to any penalty for failing to comply with a collection of information if it does not display a currently valid OMB control number.
PLEASE DO NOT RETURN YOUR FORM TO THE ABOVE ADDRESS.

1. REPORT DATE *(DD-MM-YYYY)* 30-JUN-2012	2. REPORT TYPE Thesis	3. DATES COVERED *(From - To)* 18-JUL-2007 -- 18-MAR-2011

4. TITLE AND SUBTITLE Determining the Infectious Dose of Influenza Aerosols in a Mouse Model	5a. CONTRACT NUMBER FA8650-07-C-5911
	5b. GRANT NUMBER
	5c. PROGRAM ELEMENT NUMBER 0909999F
6. AUTHOR(S) McDonald, Rashelle S.	5d. PROJECT NUMBER GOVT
	5e. TASK NUMBER L0
	5f. WORK UNIT NUMBER Q230L7BD

7. PERFORMING ORGANIZATION NAME(S) AND ADDRESS(ES) Student at the University of Saint Joseph—Connecticut 1678 Asylum Avenue West Hartford, CT 06117-2791	8. PERFORMING ORGANIZATION REPORT NUMBER

9. SPONSORING/MONITORING AGENCY NAME(S) AND ADDRESS(ES) Air Force Research Laboratory Materials and Manufacturing Directorate Airbase Technologies Division 139 Barnes Drive, Suite 2 Tyndall Air Force Base, FL 32403-5323	10. SPONSOR/MONITOR'S ACRONYM(S) AFRL/RXQL
	11. SPONSOR/MONITOR'S REPORT NUMBER(S) AFRL-RX-TY-TP-2012-0062

12. DISTRIBUTION/AVAILABILITY STATEMENT

Distribution A: Approved for public release; distribution unlimited.

13. SUPPLEMENTARY NOTES

Ref Public Affairs Case # 88ABW-2013-0292, 23 January 2013. Document contains color images.

14. ABSTRACT

An animal model system was developed for measuring the infectivity of aerosol challenges delivered to mice via a nose-only bioaerosol device. The measured dimensions of the first organism evaluated, *Francisella tularensis* LVS, was found in initial experiments to be considerably larger than its reported proportions, which eliminated it as a candidate for animal aerosol filtration and respiratory exposure studies. Influenza A/PR/8/34 (H1N1) was selected as a replacement and its aerosol characteristics were found to be satisfactory for filtration studies. After a direct inoculation experiment demonstrated susceptibility to three strains of mice, the Controlled Aerosol Test System was used to deliver a series of graduated doses of this virus by inhalation to groups of five 25-g female CD-1 mice, from which a median infective dose (MID_{50}) of less than 40 $TCID_{50}$ was inferred from weight loss, and a lower-limit value of ~ 12 $TCID_{50}$ was calculated from cytopathic effect and qRT-PCR data. The method demonstrated in this study can be used to further the development of rodent models for evaluating aerosol delivery of pharmaceuticals and technologies for infectious disease control, and to create and validate computational models for aerosol delivery. In addition, the original work of evaluating the efficiency of respiratory protection equipment from infective particles of penetrating particle sizes can now be completed.

15. SUBJECT TERMS

animal model, bioaerosol, BALB/c, C57BL, CD-1 mouse, H1N1, infection, influenza, inhalation, respiratory

16. SECURITY CLASSIFICATION OF:			17. LIMITATION OF ABSTRACT	18. NUMBER OF PAGES	19a. NAME OF RESPONSIBLE PERSON Joseph D. Wander
a. REPORT	b. ABSTRACT	c. THIS PAGE	UU	70	
U	U	U			19b. TELEPHONE NUMBER *(Include area code)*

Reset	**Standard Form 298** (Rev. 8/98) Prescribed by ANSI Std. Z39.18

Determining the Infectious Dose of Influenza Aerosols in a Mouse Model

by

Rashelle S. McDonald

A Thesis

Presented to the Faculty of the University of Saint Joseph

in partial fulfillment

of the requirements

for the degree of

Masters of Science

in the department of

Biology

June 20, 2012

This thesis by Rashelle S. McDonald
is accepted in its present form
by the Department of
Biology

as satisfying the thesis requirement
for the degree of Master's of Science

12/10/12

Date

Director of Thesis (Christopher R. Zito, Ph.D.)

12/10/12

Date

Thesis Committee Member (Charles Morgan, Ph.D.)

13 Dec 12

Date

Thesis Committee Member (Steven Goldstein, Ph.D.)

10 Jan 13

Date

Thesis Committee Member (Joseph D. Wander, Ph.D.)

Date

Academic Dean (Daniel Nussbaum, Ph.D.)

Acknowledgements

There are so many people who deserve my heartfelt gratitude for helping me during my research and writing of this document. First and foremost, with God all things are possible (Phil 4:13). My family, friends and coworkers have been very supportive and instrumental in my work and without their love and not so gentle prodding, I never would have gotten this far and although I cannot possibly list you all by name, you know who you are. There are a few special "thank yous" I want to mention: Bob Nichols was an influential source for design and technical advice throughout this project and personally for helping me keep my head above (and under) wa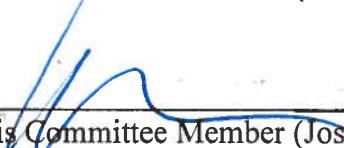ter. I truly appreciate the patience of Dr. Joe Wander, Dr. Jeff Owens and Brian Heimbuch and for allowing me the time and providing direction to complete this research. My advisor, Dr. Charles Morgan of USJ also deserves my gratitude for his patience and assistance in this process. I must also acknowledge all of the hard work and collaboration of my friends at the University of Nebraska Medical Center. The donation of eggs from Pilgrim's Pride Hatchery, Live Oak, FL, was crucial to performing this research and is much appreciated. I would like to dedicate this work to my dear friend who departed this earth before I completed this work; Ryan always encouraged me to work hard and produce this written work.

So without further ado, I present to you the "Thesis of the Mices":

TABLE OF CONTENTS

Abstract

Determining the Infectious Dose of Influenza Aerosols in a Mouse Model

2012

Rashelle McDonald

Charles Morgan, PhD.

An animal model system was developed for measuring the infectivity of aerosol challenges delivered to mice via a nose-only bioaerosol device. The measured dimensions of the first organism evaluated, *Francisella tularensis* LVS, was found in initial experiments to be considerably larger than its reported proportions, which eliminated it as a candidate for animal aerosol filtration and respiratory exposure studies. Influenza A/PR/8/34 (H1N1) was selected as a replacement and its aerosol characteristics were found to be satisfactory for filtration studies. After a direct inoculation experiment demonstrated susceptibility to three strains of mice, the Controlled Aerosol Test System was used to deliver a series of graduated doses of this virus by inhalation to groups of five 25-g female CD-1 mice, from which a median infective dose (MID_{50}) of less than 40 $TCID_{50}$ was inferred from weight loss, and a lower-limit value of ~ 12 $TCID_{50}$ was calculated from cytopathic effect and qRT-PCR data. The method demonstrated in this study can be used to further the development of rodent models for evaluating aerosol delivery of pharmaceuticals and technologies for infectious disease control, and to create and validate computational models for aerosol delivery. In addition, the original work of evaluating the efficiency of respiratory protection equipment from infective particles of penetrating particle sizes can now be completed.

Development of a Mouse Model for Evaluation of Respiratory Protective Equipment

Introduction
Respiratory Protection

The baseline defense against infection by airborne pathogens and particulate air toxic materials is a respirator. For such respiratory protection equipment (RPE) to be useful, it has to capture or neutralize particles, both inert and biologically active, before they enter the wearer's respiratory tract while still allowing the wearer to breathe well enough to perform regular work tasks. A study of the benefit from the antimicrobial agent is beyond the scope of this project, but it remains a goal for the future of respiratory protection.

The risk of viral or bacterial penetration through a filter has implications in a variety of realms, including medical professionals, emergency response teams and the military. The ideal protection device against biological organisms would be an impenetrable surface that no organisms can break through. When working with air filtration, however, this is not feasible. Air filters with tight weaves, such as HEPA (high efficiency particulate air), are efficient but impose large pressure drops that are exhausting to the user because of the effort required to get air through. This makes them less desirable to use and leads to user non-compliance.

Most fielded military RPE utilizes HEPA filters because they are 99.97% efficient at removing 0.3-μm particles, and are pretested with sodium chloride (NaCl) or dioctyl phthalate (DOP) to validate performance (Moyer and Stevens, 1989). While 99.97% is very good, a challenge of 10^6 particles could yield a penetration of 300 particles. This is especially significant when dealing with biological particles that have a minimum infectious dose (MID) of well below 300 particles. While most bacteria are larger particles (0.50 to 5.0 μm) ranging widely with most falling in a

range of 10^3 to 10^7 colony-forming units (CFU) to reach levels that are considered infective there are some bacteria, such as *F. tularensis* that can cause infection with single numbers of bacterium. It is thought that for many of the bioweapons, viruses (0.05 to 0.3 microns in size) with an MID of <100 plaque-forming units (PFU) (Franz, 1997) are more likely to penetrate protective filters thus causing infections. Therefore the HEPA filter alone may not be adequate to protect the user from infection when challenged with high loads of specific bacteria or even small loads of most viruses.

There are numerous problems associated with evaluation of RPE filters. In vitro experiments and modeling are helpful but do not describe what happens to biologically active particles that enter a host or the effect on the RPE itself. There are many interactive surfaces in the mammalian respiratory tract that can change the way a microbiological particle will react once in contact with it. Impinger capture is incomplete (Hogan, 2005) and assay methods may not be sensitive enough to tell the whole story or can even provide misleading information (Ali, 2011). The most challenging RPE articles to evaluate are those that claim to act as antimicrobials against penetrating bioaerosols. The use of an animal model has been proposed (Stone et al., 2012), and this project sought to identify a suitable pathogen–animal pair to support a demonstration of this concept.

Section I—Aerosol Device Design and *Francisella tularensis*

Background

Experimental inhalation exposure systems are an established investigational tool and the subject

of several reviews (Cheng and Moss, 1995; Drew and Laskin, 1973; Jaeger et al. 2006;

MacFarland, 1983; Wong, 2007). The purpose of this study was to identify and evaluate a mouse

model as a complement to a measured-dose bioaerosol delivery apparatus termed CATS

(Controlled Aerosol Test System) for measuring the clinical significance of media used in

respiratory protective equipment (RPE). The mice serve as a detector to evaluate the clinical

effect of articles of RPE by directly observing the change in infectivity the protective article

evaluated causes by data measured post exposure and post mortem.

A nose-only inhalation exposure system (NOIES) was chosen primarily to prevent transmission

of ophthalmic and enteric infections to the mice. The aerosol enters the CATS, then goes through

the 12-port, directed-flow, NOIES before exiting the test system through the high-efficiency

particle arresting (HEPA)-filtered exhaust. The capacity of the nose-only rodent exposure system

to deliver infectious aerosols to mice was validated and verified by Jaeger et al. (2006). Total

flow rate through the system was regulated at the Collison to deliver 2.0 ± 0.1 liters per min

(LPM) measured on exit by a mass flow meter (TSI Model 4043E). A rotating joint inserted at

the inlet to the mouse tree allows it full range of rotation and makes all the sockets accessible

inside the tight spaces of a biological safety cabinet (Baker Company, Sanford, ME; SG603-

ATS) to confine generated aerosols.

The primary goal of the combined project was to design an aerosol device that could be

employed using a diverse array of organisms and have those organisms remain viable throughout

the aerosolization process so the end host animal model can serve as an effective indicator of

penetrating infectivity/clinical benefit of the RPE tested. Some problems encountered in similar research include irreproducible results and wide variation between labs so that data cannot be compared among researchers. It was important to evaluate the system with several different aerosols—each exhibiting different characteristics—and to note particle size distribution (PSD). PSDs of inert (salt and polystyrene latex) and biological aerosols were shown to be consistent within runs and reproducible from run to run (Stone, 2010).

The proposed animal exposure study was both enabled and made necessary by coupling an aerosol delivery device to an animal exposure system through an intermediate vessel to support an air treatment technology—CATS (Stone, 2010 and Stone et al., 2012). CATS provides a tool to measure protection against infection by aerosolized pathogens delivered through the system and filter to be tested. To achieve this measurement, we must deliver an accurate, known dose of infective agent to each animal at a consistent concentration C and PSD for a series of selected time periods t; we chose to run the system for up to two hours to account for both impinger collection parameters and animal exposure time points. Varying C for each run (which includes several values of t) fills out the dose/survival curve. As the aerosol device was being configured, my task was to select an organism to aerosolize for the study.

Francisella tularensis is a Gram-negative, facultative intracellular bacterium and the causative agent of tularemia (Chen et al., 2005). Tularemia is an infection that humans and other mammals can contract; clinical manifestations vary with contraction method. *F. tularensis* is grouped among the most harmful bacterial agents and have potential to be used as Category A biological warfare agents, a designation that includes the causative agents for anthrax, plague, and viral hemorrhagic fevers. *F. tularensis* is an endemic bacterium in many geographic locales, including North America, Europe, China and Russia; a variety of subspecies occur throughout these

regions. *F. tularensis* can withstand a variety of temperatures, including moist heat (121 °C for at least 15 min) and dry heat (160–170 °C for at least 1 hour); this bacterium also remains viable at freezing temperatures (as low as -15 °C) for months to years (CFSPH, 2007). A small number (approximately ten; Conlan et al., 2003) of *F. tularensis* organisms can infect a person, often fatally, which is one of the qualities this bacterium possesses that make it an interesting organism to study. Couple its ability to remain infective in the environment for several weeks, its transmission by ingestion or exposure to aerosolized body fluids from arthropod hosts to animals or humans and from animals to humans, its ability to be easily aerosolized, and its tendency to cause a variety of clinical manifestations in humans and *F. tularensis* appears to be an ideal organism for studying aerosol transmission through respiratory protection devices. Even though this organism is considered highly infective and dangerous, person-to-person transmission is undocumented, suggesting that the bacteria are not aerosolized from the respiratory tract. Because of this limited risk of secondary infection, it was considered acceptable to economize by co-housing mice in their exposure groups.

Bergey's manual (1984) reports the growth of *F. tularensis* to be relatively slow; incubated at 37 °C it reportedly takes up to 14 days to grow on chocolate agar or cysteine heart agar plates. Bergey's manual (1984) describes *F. tularensis* as a semi rod-shaped bacterium, sometimes coccoid, at a size of 250 nm x 700 nm (0.25 μm x 0.7 μm), which is near the most-penetrating particle size for a HEPA filter (designed to capture 99.97% of 0.3-μm particles)—a dimension that suggests significant potential for delivery as an aerosol weapon. Our scope of interest includes evaluation of RPE and clinical significance of chemically treated filters against such particles. The reported size and characteristics of *F. tularensis* describe an organism ideal for a study of bioaerosol RPE penetration and infectivity post penetration using a live animal model.

The broad clinical manifestations include predominately three forms: cutaneous, respiratory and enteric infection. The good news about a typical *F. tularensis* infection is that, if recognized in time, it is treatable with common antibiotics, including streptomycin, tetracycline and chloramphenicol. The bad news is that its being treatable makes it a more effective threat because the time and resources to treat an infected patient are much greater than the effort to simply bury his remains. Prevention would be more practical than treating large numbers of infected patients and much more desirable than a high death toll. Receiving newfound publicity, NIAID (National Institute of Allergy and Infectious Diseases) deems the aerosolized version of *F. tularensis* dangerous enough to merit a drastic increase in the budget for tularemia vaccines and NIH (National Institutes of Health) also increased the number of funded projects on *F. tularensis* (Relman, 2006). Some aerosol work has been performed utilizing mice receiving aerosolized doses of *F. tularensis* (Conlan et al., 2003; Chen et al., 2004; Twine et al., 2006); all show that various mice are susceptible to aerosolized *F. tularensis* in relatively low doses.

A vaccine is available for *F. tularensis*, derived from an attenuated strain of the bacterium termed the live vaccine strain (LVS). LVS is less harmful to humans, but lethal to several strains of mice (Conlan et al., 2003), so this strain is suitable for use in the laboratory with mouse models that exhibit a clinical response to it. LVS is listed as a BSL-2 organism, but when an organism is aerosolized, the ASHRAE (American Society of Heating, Refrigeration, and Air-conditioning Engineers, Inc.) guideline is to use the next-higher containment level, so a BSL-3 facility was necessary. Because laboratory animals were involved, an ABSL-3 facility was required (BMBL, 2009). All standard safety protocols were followed in the course of our work with LVS. It proved fortunate that an initial characterization study was undertaken to familiarize ourselves with LVS and LVS aerosols prior to starting expensive animal exposure studies.

Methods and Materials
Exposure System Description and Operation

An apparatus was designed, constructed and validated (Stone, 2010; Stone et al., 2012) to deliver

a precisely measured aerosol concentration, either directly or after passage through a filter

medium, through a *Nose-Only* Directed-Flow Inhalation Exposure System (NOIES, CH

Technologies, Westwood, NJ; Jaeger et al., 2006) to individual mice (Figure 1). This low-flow,

single-pass design consists of an aerosol generator, diffusion drier, charge neutralizer, filter

holder, sampling ports and NOIES unit (Stone, 2010; Stone et al., 2012). The entire system is

termed the CATS. The CATS generates a biological aerosol over a range of constant

concentrations and, after conditioning and treatment—if any treatment is applied—delivers the
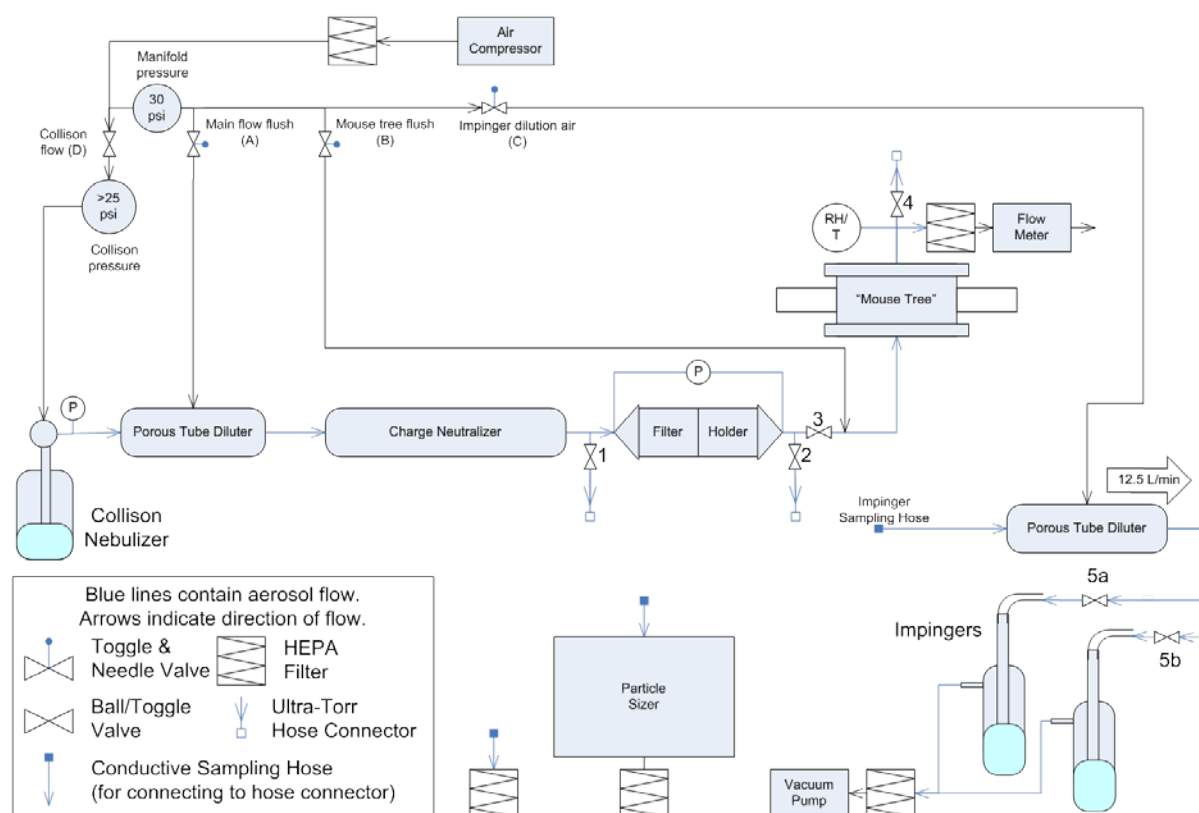
Figure 1. Schematic of the controlled aerosol test system (CATS). The CATS allows data for

both concentration and viability to be collected within the same data collection series.

concentrations and, after conditioning and treatment—if any treatment is applied—delivers the particles to the nose of a mouse constrained in a polycarbonate tube (CHT-247, CH Technologies) as a pure respiratory exposure.

The main system components were connected using 0.5-inch (12.7-mm) stainless steel tubing with a minimum number of gradual bends. In operation, a single-jet Collison nebulizer (BGI Inc., Waltham, MA), regulated to 25–30 psi was used to atomize the inert and viral suspensions. The aerosol passed through a 9.5-inch (23-cm) diffusion drier and then through a 2-mCi ^{85}Kr charge neutralizer (TSI Inc., Shoreview, MN) to restore a Boltzmann equilibrium charge distribution. After passage through the filter holder the aerosol enters the 12-port NOIES before exiting the test system through the HEPA-filtered exhaust. Total flow rate through the system was regulated at the nebulizer to deliver 2.0 ± 0.1 LPM measured on exit by a mass flow meter (TSI Model 4043E). The entire system was designed to fit inside a biological safety cabinet (Baker Company, Sanford, ME; SG603-ATS) for additional protection from generated aerosols. The unique feature of the system is an optional filter holder (Triosyn Corp, Williston, VT), which is capable of holding filter media samples 47 mm in diameter. Smaller discs of filter media can be accommodated with the use of reducers. To validate the CATS, Stone (2010) and Stone et al. (2012) demonstrated uniform distribution of salt and PSL aerosols across the ports of the NOIES.

Uniformity of Bioaerosol Distribution to Test System Ports

Collections of 250-nm and 1-µm PSL beads were accomplished by inserting the sampling tube of the SMPS or APS in separate exercises into the tip of a mouse restraint device and installing the tube into a socket of the NOIES at each of the 12 ports; the mean particle count from each

port was read via the particle sizer then calculated at each aerodynamic size and compared. We then relocated CATS to UNMC. After installation in the ABSL-3 cabinet at UNMC, the CATS was challenged with a water aerosol and then with sodium chloride solution to verify that its performance had not been compromised during disassembly, transportation and reassembly. The APS was used to read the PSD of water aerosols from each of the 12 ports in triplicate.

As *F. tularensis* is listed as a select biological warfare agent and its use requires certification, a surrogate was needed to proceed with initial data collection. *F. philomiragia* (a nonpathogenic surrogate for *F. tularensis*) purchased from ATCC (American Type Culture Collection, Manassas, VA) #25015 was thawed and suspended in trypticase soy broth (TSB) (BD BBL, Becton Dickinson and Company, Franklin Lakes, NJ), then plated in triplicate on BBL chocolate II agar plates (Lot# S100077/2112/20080806) and grown overnight at 37 °C. Plates were transferred to get three ages of bacterial growth on plates—6-, 9-, and 17-day-old colonies. All were examined under a regular light microscope and the average size and general shape were recorded.

To determine if the *F. philomiragia* subspecies was an atypically large subspecies of the bacterium, a gamma-irradiated *F. tularensis* LVS (CRP–Critical Reagents Program, Frederick, MD) was obtained for further size characterization. The strain was observed under oil using a 100X immersion microscope lens (Figure 2). The particle size was also evaluated as an aerosol, using the APS (TSI, Shorview, MN). The aerosolization medium was sterile water as we were not concerned with viability of the bacterium and wanted a true size measurement.

We were not able to perform viable penetration experiments with *Francisella* sp. due to the BSL limits of our lab. A collaboration was instituted to work with LVS at the University of Nebraska Medical Center (UNMC) to show viability of aerosolized *F. tularensis* over time (0, 60, 90 and
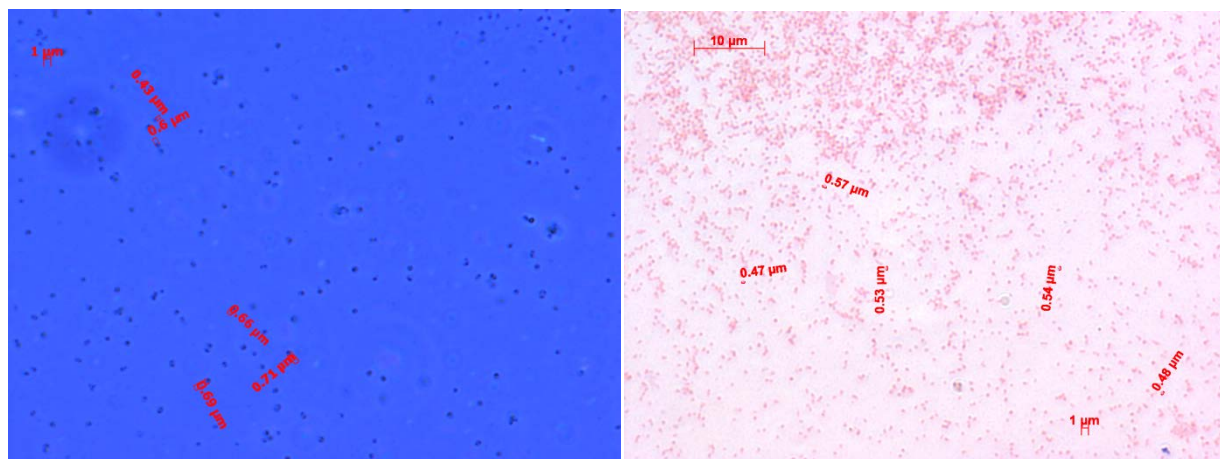
Figure 2. Left—Image of γ-irradiated *F. tularensis* LVS (from CRP) shown at100x. The average

size is 0.62 μm. Right—Image of Gram-stained *F. tularensis* LVS, average size 0.52 μm.

120 mins) as well as the effect on viability of various aerosolization media (0.1% peptone, 0.5%

raffinose, both in water, and an unbuffered aqueous medium), to learn growth characteristics, and

to measure penetration of LVS through filter media. Aerosol samples were collected downstream

into 1X PBS (Fisher, Pittsburgh, PA) in all-glass impingers (AGI-30, Ace Glass, Vineland, NJ).

To identify a suitable buffer, plates of *F. tularensis* LVS were grown up to confluent lawns for

48 hrs at 37 °C and 5% CO_2, then scraped and rinsed in 6 mL 1X PBS. Serial 1:10 dilutions were

made in each of three buffer solutions: 0.1% peptone, 0.5% raffinose, and an unbuffered aqueous

medium and held in the respective media for 0, 60, 90 or 120 mins to evaluate stability of the

organism in the buffer. The optical density (OD) was read (SmartSpec Plus, Bio-Rad

Laboratories, Philadelphia, PA) and recorded at 580, 600 and 625 nm, and differences before and

after aerosolization were noted. Chocolate agar plates were made from collections at these same

time points and the plates incubated 48–72 hrs under standard growth conditions (Figure 3).
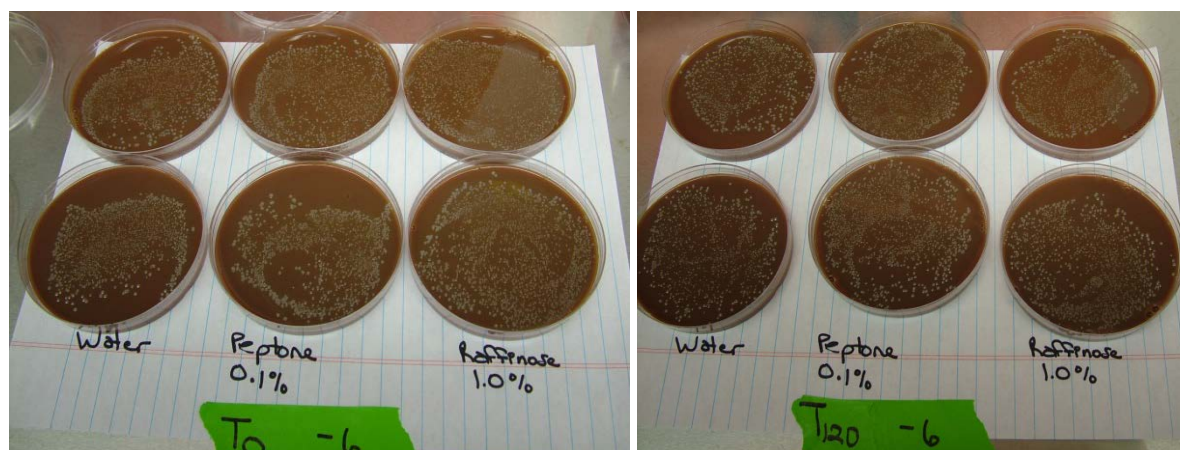
Figure 3. *F. tularensis* LVS growing on chocolate agar plates. Left is t_0 in each of three buffers; Right $t_{120 \text{ mins}}$). No difference in the viability of *F. tularensis* is visible among these three media.

 In preparation for the aerosol run all three aqueous media above were prepared and 6 mL of each was placed separately in a single-jet Collison nebulizer first without a *F. tularensis* culture, then with the growth recovered from plates of *F. tularensis* LVS incubated overnight. A simplified version of the CATS was assembled, comprising a Collison nebulizer, ^{85}Kr charge neutralizer, upstream sampling port, filter holder, downstream sampling port and HEPA-filtered exhaust.

Results
Sampling Validation

The particle counts at each port were averaged and again seen to be uniform within 10% (data not shown). A subsequent delivery of 100 mg/L sodium chloride (NaCl) in water showed PSD to vary $\leq$ 7% between all port replicates. Figure 4 plots the coefficient of variation (CV) as a function of particle size at the 12 ports for the NaCl aerosol measurements. The consistency was

calculated based on the combined concentration at the aerodynamic diameter at which the peak

occurred and at the two surrounding data points (Stone 2010).
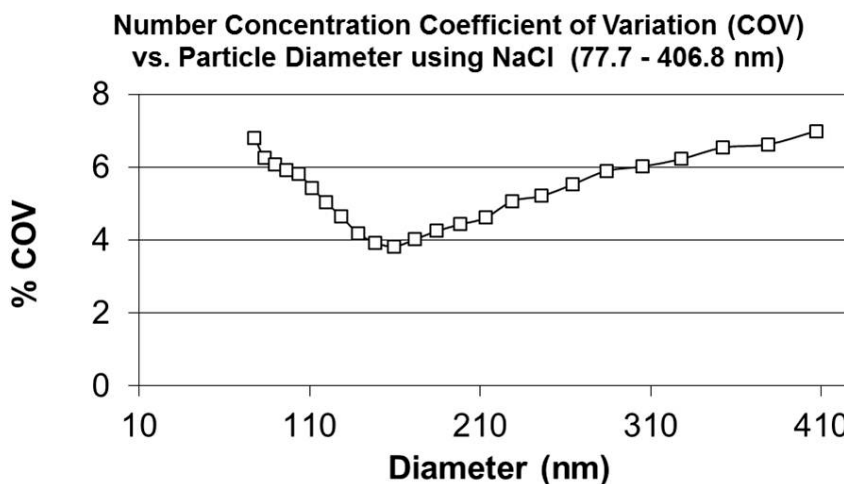
Figure 4. Port validation of the CATS using sodium chloride aerosol.

Once port correlation was verified, the particle size distribution could be verified, also using the

sodium chloride solution. Samples were taken in triplicate from the sampling port located

downstream of the NOIES. Results indicated that the aerosol was polydisperse with a number

mean diameter of 74 nm and the mass mean diameter of 208 nm over the range of particle

diameters from 10–407 nm (Figure 5).
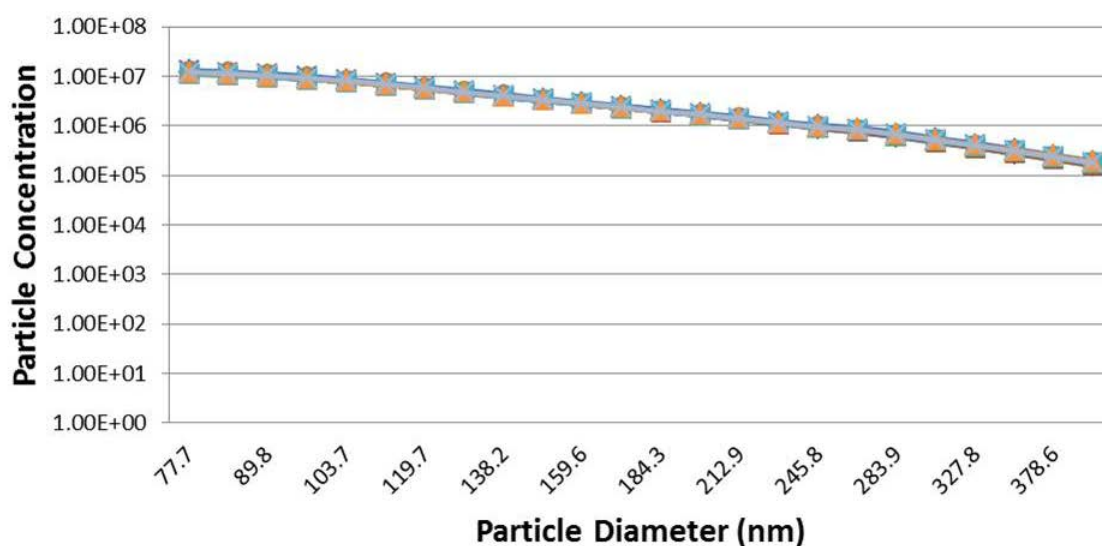
Figure 5. Particle size distribution of sodium chloride aerosol.

F. philomiragia was observed under the microscope at three ages (6, 9 and 17 days) to have a coccoid shape and an average diameter of 0.83 μm—*three times* the value reported (Bergey's, 1984) for *F. tularensis*. Aerosolization of *F. philomiragia* in 1X PBS produced particles that the APS measured to be larger than 0.50 μm. When both analytical methods revealed an average size larger than Bergey's (1984) reported, a modified Mueller–Hinton broth growth medium was recommended (personal communication, Peter Iwen, PhD. Public Health Laboratory, UNMC, Omaha, NE) to decrease the bacterial size. However, the dimensions of the culture grown in the Mueller–Hinton medium were only slightly smaller.

Optical density (OD) was read and recorded at 580, 600 and 625 nm before and after aerosolization in both the unbuffered aqueous medium and 0.1% peptone using a UV–visible spectrophotometer. Although it is understood that neither the particle sizer nor the UV–visible spectrometer is able to detect viability of bacteria, both are simple detection methods that can be used to determine trends or differences in the samples. For the OD data, the differences before

and after aerosolization remained small in the 0.1% peptone medium. Differences in OD pre and post aerosolization in the unbuffered medium were larger (12–35% decrease), leading us to believe that a negative effect, possibly cell death, caused the lower OD following aerosolization in the unbuffered medium.

Discussion
Both aerosol concentration and viability pre and post filtration are of importance when evaluating bioaerosol penetration through filter materials. Variation in aerosol delivery between ports and particle size distribution were important factors in the validation of the CATS. Experiments were conducted to look for variation among the NOIES ports in the concentration of particles delivered over a unit of time. Stone et al. (2012; Stone, 2010) demonstrated uniform distribution of an aerosol to several ports of the CATS using various sized particles. Following installation of the CATS the exposure system was retested to verify consistency of particle counts among all 12 ports, using tap water and sodium chloride solution to generate test aerosol particles. Stone et al. (2010) was able to determine the loss of particles within the system, and to ensure that samples from different ports can be compared with one another.

The ability of three buffer solutions to sustain LVS over the course of an aerosol run was evaluated. The particle size of each medium alone was evaluated before *F. tularensis* LVS was added to the Collison nebulizer. Particles from the raffinose medium were ~1.5 times as large as those from the peptone medium (Figure 6), so the larger raffinose particles were eliminated from further study—the efficiency of exclusion of particles by a filter medium increases rapidly as their size grows above the MPPS (most penetrating particle size).
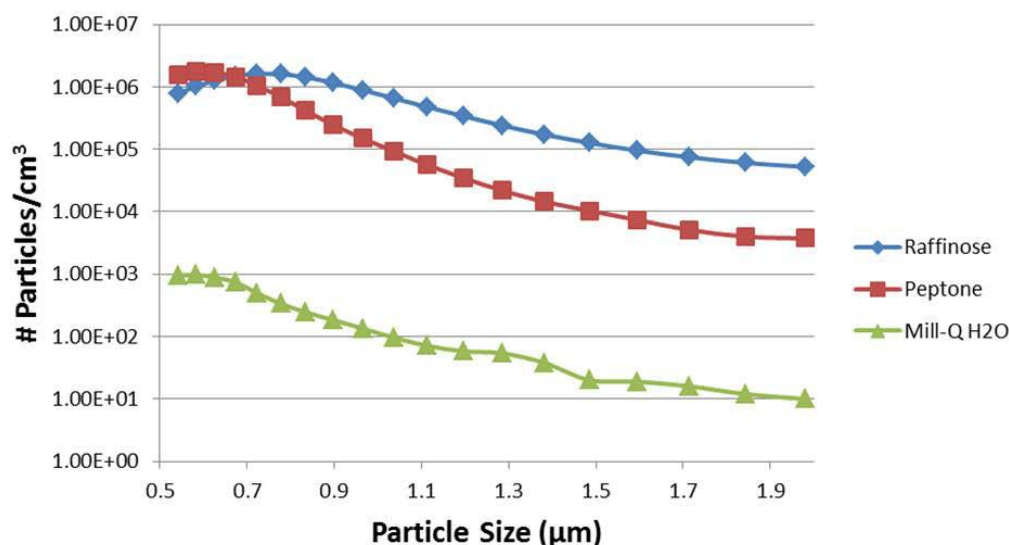
Figure 6. APS counts of the particle size distribution from three media, from which one was to be selected for aerosolizing *F. tularensis* LVS.

Contrary to the 250-nm diameter reported in Bergey's manual (1984), we found *F. tularensis* LVS to exist in liquid culture (modified Mueller–Hinton broth) and on chocolate agar plates as 600~800-nm (0.6~0.8-μm) spheres. This is *much* larger than the reported size and delivery from a sugar or protein buffer (raffinose and peptone, respectively) will create huge particles that should be expected to occlude the filter medium in minutes. An unbuffered aqueous medium was also evaluated for aerosol transport of *F. tularensis* LVS; Figure 7 shows that the mean aerodynamic diameter measured by the APS from aerosolization of the bacterium in peptone was ~50 nm larger than from the unbuffered medium. The OD was also measured to determine if any changes occurred during the aerosolization process. There was a larger reduction in the OD from samples in the unbuffered medium. Although this cannot directly relate to viability, it must be

considered highly probable that *F. tularensis* will not withstand aerosolization without some buffer added.
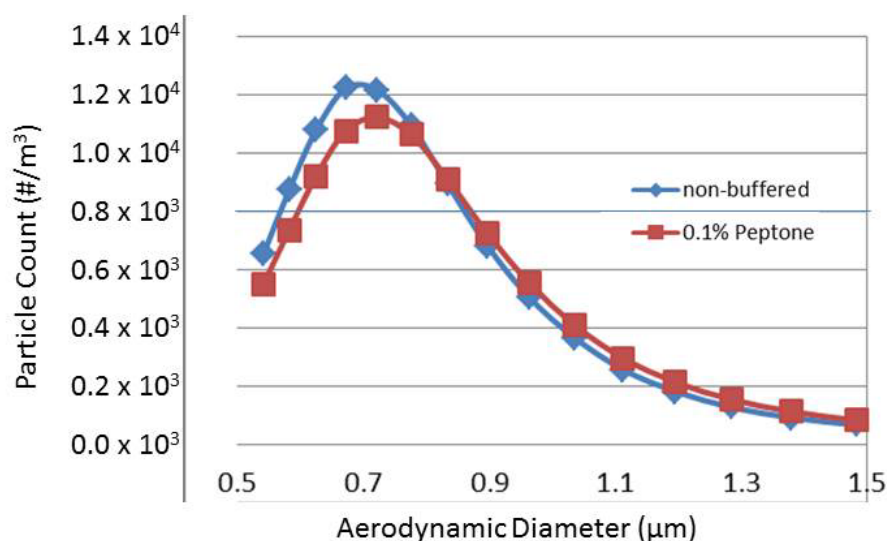
Figure 7. Plot from the APS of particle size distributions of *F. tularensis* aerosolized in an unbuffered aqueous medium and in water containing peptone.

The larger size of the *Francisella* spp. plus the requirement to increase the particle size by delivery from a supportive medium functionally eliminated this genus as candidate test organisms. The mismatch of sizes was not further evaluated at this time, but may be due to staining and preservation techniques used. A positive finding was that *F. tularensis* LVS grows quicker than originally expected; it took only two days to get countable colonies to work with after incubation at 37 °C instead of the originally reported 14 days (Bergey 1984).

As the *Francisella* spp. were too large to penetrate the HEPA medium in reliably countable quantities to support the target filter penetration measurements, it became necessary to select a different pathogen with sufficient intrinsic visibility to be of general interest.

Section II- Influenza and Mice

Background

Influenza illness is often associated with occurrences of annual or near-annual epidemics in temperate climate zones. Exposure to influenza virus often leads to a disease presenting as an acute and temporarily incapacitating infection of the upper respiratory tract. The range of illness resulting from influenza virus spans from asymptomatic infection to mild symptoms to often fatal pneumonia. Those most often affected are the young, elderly or immunocompromised (Hayden, 1997). Factors such as the strain of influenza virus that caused the illness, immune status of the host, and/or age of the affected individual play an important role in recovery or progression of disease. This was evident in the 2009 outbreak of influenza with the Influenza A virus H1N1 pandemic (pdm) strain, during which a disproportionately higher percentage of morbidity occurred in children and young adults as well as in individuals with such underlying conditions as obesity or diabetes (Jhung et al., 2011). The influenza A (H1N1) virus selected for this study was chosen based on reports of its infectivity in mice (Smee et al., 2008)—even though it had not been mouse adapted—and its known hardiness in culture systems as a starting point for development of a mouse model for aerosolized influenza. The size (80~120 nm) of this entity is also compatible with the experimental design and aims.

Influenza is considered a communicable disease, although the leading methods of transmission are still being evaluated (Brankston et al., 2007; Lee, 2007; Lemieux and Brankston, 2007; Tang and Li, 2007; Tellier, 2006; 2007a; 2007b). Coughs and sneezes that create droplet nuclei are expected routes of infection in addition to the virus coming in contact with mucus membranes. The emergence of avian influenza has brought the disease to the attention of the mainstream

population and has researchers more engrossed in finding methods of transmission, protection, prevention and cures.

Travel is prevalent and far-reaching and is often a necessity of current society. Along with the increase of travel has come the rise and spread of disease-causing microorganisms—even those previously considered nearly eradicated—and the spread is occurring faster and further, resulting in secondary infections to those populations previously considered not at risk (Gautret 2012). Because of influenza's ability to reassort based on surface proteins (antigenic drift), the risk is that the recombination of genetic material from these diverse circulating viral subtypes will cause a more serious antigenic shift. Pandemics are infrequent but often severe events due to the creation of novel, unpredictable strains of influenza A virus (Treanor, 2004) caused by antigenic drift, which can lead to a new viral subtype. Once a new viral subtype is created, the host's immune response can no longer recognize and mount a response to the new virus. When the new viral subtype introduced to the human population and is infective antigenic drift can occur. This ability to jump from one species into another, potentially naive species (e.g., avian influenza) and cause a large proportion of influenza-related deaths across multiple species is the potential for a new pandemic. Influenza is considered a fastidious virus (because of its viral envelope) and it has a unique ability to mix or reassort, even within a host, which can lead to a wide variety of subtypes, making influenza difficult to contain or control. Within the last 100 years influenza pandemics have occurred four times (1918 (H1N1), 1957 (H2N2), 1968 (H3N2) and 2009 (H1N1)) (Oxford, 2000).

Animal models

A number of animal models have been studied to evaluate new vaccines and other approaches for preventing influenza-related disease (Gubareva et al., 1998; Ng et al., 2010), but vaccines are only one form of protection. Once the virus circulates among a population, other preventative measures are necessary to shield people; here the focus is on RPE. The CDC has collaborated with OSHA, NIOSH and USDA to determine the level of protection appropriate during such pandemics (CDC, 2012-A). NIOSH is the leading authority for regulations regarding the use of RPE. One main public health concern is that, when the next pandemic strikes, there will be a shortage of vaccines and protective masks and an overload on healthcare clinic resources. Although the CDC reported that the 2011–2012 flu season experienced fewer than the anticipated number of influenza-related illnesses, there is no reason to expect that trend to continue for upcoming seasons (CDC, 2012); the public health community is already making plans for another pandemic (Bailar et al., 2006).

Although numerous mathematical models have been developed to calculate particle deposition within the respiratory tract, predicted results are unable to account for all scenarios possible in *in vivo* measurements, especially when characterizing the effects of disease. Carefully chosen animal models allow closer approximation to a human response and therefore it is important to continue to further develop these models.

We sought to establish an animal aerosol exposure model in which air filtration media can be evaluated using live animals rather than impinger capture as indicators for attenuation of infectivity. For more than 75 years laboratory mice have served as models for susceptibility to and pathogenesis of influenza disease (Andrewes et al., 1934). Their comparatively low cost,

small size and relative susceptibility to the virus make mice an ideal candidate for studying influenza virus infections. The mouse is currently considered the primary model for the evaluation of influenza antiviral agents because it is a predictive indicator that mimics the complexity of the human system and response to disease (Sidwell and Smee, 2004), and the emergence of new pandemic subtypes of influenza A has elicited calls for more-intensive study of influenza (Beigel and Bray, 2008).

Materials and Methods
Propagation of Virus

Influenza A/PR/8/34 (H1N1) virus was obtained from American Type Culture Collection (Rockville, MD) as frozen stock (ATCC VR-1469). Virus was propagated in chicken eggs using CDC Unit 15G.1 protocol (Szretter et al., 2005). Titers were performed and calculated using the Spearman–Kärber method (Armitage and Allen, 1950; Bross, 1950; Finney, 1964).

Prior to growing the H1N1 virus, transmission electron microscopic images of H5N1 (due to its lab availability) were taken to confirm the generic size of the influenza virus (Figure 8). No size difference was expected between H5N1 and H1N1, as only the hemagglutinin and neuraminidase surface proteins differ between the two subtypes. Influenza is visible to the DoD community as a potential biowarfare agent, but has higher current (and recurring) relevance to the public health community, witness the avian influenza scare of 2009. The availability of a human vaccine attenuates the slight risk of working with a moderate human pathogen, so it was decided to conduct a test of the viability of H1N1-PR8 dispersions in DI water in the nebulizer reservoir and in aerosols caught in AGI-30 impingers. Loss of viability measured at UNMC was minimal so we revised the test plan to substitute H1N1 for *F. tularensis* and undertook the training needed to secure approval for animal use.
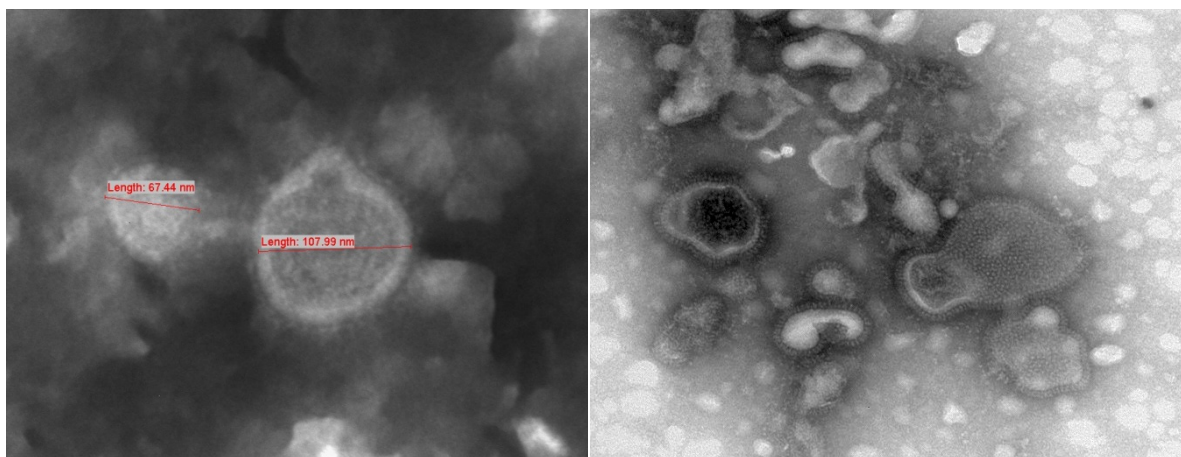
Figure 8. Transmission electron microscope images of H5N1. Courtesy of Michael Lore, UNMC. Note the size of the virion between 67.44 nm and 107.99 nm.

Particle Size Distribution of Influenza Aerosols

To assess the particle size distribution (PSD) of aerosols containing influenza virus, samples were taken in triplicate from the sampling port located downstream from the CATS and read using the SMPS.

Animal husbandry/groupings

Prior to starting experiments a power analysis was calculated using the PASS software to determine the number of mice necessary to detect a statistical difference between a control group of mice and group of mice exposed to aerosols.

Three strains of female mice (C57BL, BALB/c and CD-1) were purchased from Charles River Laboratories (Portage Facility, MI). The mice were 6–8 weeks old and ranged in weight from 18–30 g. Mice were randomly divided into groups assigned to specific exposure time points, and

no more than five (all in a given exposure group) were housed per cage. Animals were provided

rodent chow (Harlan Teklad, U.S.) and water *ad libitum* and maintained on a 12-hr light/dark

cycle. All animal work was carried out in an ABSL-3 facility following institutional and

regulatory procedures. To minimize artifacts caused by stress during respiratory exposure

sessions, mice were preconditioned daily during the week preceding their exposure sessions by

insertion into a mouse restraint device (CHT-247, CH Technologies) for a period that did not

exceed the maximum exposure time for that experiment.

Infection Exposure Protocols

Intranasal Inoculation

To select a mouse strain susceptible to an influenza virus that had not been mouse adapted, we

exposed three strains of mice via intranasal inoculation with influenza virus A/PR/8/34 (H1N1).

The inoculum, consisting of 30 µL of virus at a concentration of 4.74 x 10^7 median tissue culture

infectious doses ($TCID_{50}$)/mL, was placed intranasally into each mouse. The dose was divided

equally and placed droplet-by-droplet by pipette into each naris of the anesthetized

(ketamine/xylazine) mouse. Following the same procedure, a 1:10 dilution of virus stock in 1X

PBS was used to inoculate a second set of mice of the same three strains. In all, five mice of each

strain per dilution were used to determine susceptibility to the virus. Three mice per strain were

used as controls. Each control mouse was intranasally inoculated with 30 µL total Dulbecco's 1X

PBS as previously described (Jerrells et al., 2007). Mice were weighed daily, their weights were

recorded and changes in weight were calculated.

Aerosol Exposure

Aliquots of the influenza working stock (4.74 x 10^7 TCID$_{50}$/mL concentration) were diluted to 1:30, 1:300, and 1:1000 (volume: volume ratios) in endotoxin-free water (Sigma, St. Louis, MO) to prepare concentrations aerosolized during three successive mouse exposure series described below. The single-jet Collison nebulizer was charged and allowed to run for 5 min to stabilize the system. The bypass valve directly upstream of the CATS directed the aerosol through two HEPA filters connected in series until exposure was initiated. Non-anesthetized mice were carefully immobilized in the polycarbonate tubes so that the tip of the nose projected out of an opening in the front of the holder. The tubes were then inserted securely into a port on the CATS. Once the animals were emplaced the test aerosol was directed through the system. Vents inside the cavity of the CATS directed an airstream containing the filtered aerosol at the nares of the mouse as her only source of breathing air. Excess aerosol flow and exhaled air were continuously swept away so no mouse rebreathed air from herself or another mouse.

A spread of delivered doses (proportional to concentration, C, $\times$ time, t) around each dilution was achieved by varying the time of exposure. Mice were exposed in groups for each preselected time (Tables 3–5). At the end of the exposure period the polycarbonate tubes holding the mice were removed and the next group was inserted, until all mice for that series of experiments were exposed. When time points allowed, the mice were inserted in overlapping groups. Unused ports were sealed with the supplier's standard plugs. All exposures were carried out within a biological safety cabinet. Control mice for 1:30 ($1.58\text{x}10^6$ TCID$_{50}$/mL) and 1:300 ($1.58\text{x}10^5$ TCID$_{50}$/mL) exposure groups were placed in polycarbonate tubes during the testing for a period equal to the maximum exposure time and exposed to aerosols generated from endotoxin-free water (Sigma) containing no virus. For the 1:1000 (4.74 x 10^4 TCID$_{50}$) exposure group, two sets of controls

were used. One mouse group was exposed as above, while a second group was exposed to uninfected allantoic fluid processed in the same manner as from influenza-infected eggs.

Mice were observed and weighed each of the seven days post exposure. Severely distressed mice were euthanized after the day's weighing and, following the final weighing, all surviving mice were euthanized by administration of an overdose of ketamine/xylazine by intraperitoneal injection. A necropsy was conducted and portions of the lungs were selected for molecular, histologic or viral culture assessment. Lung tissues aseptically placed into 2.7 mL of cold BD Universal Virus Transport Medium (Becton, Dickinson and Co.) were homogenized by hand using a closed ultra tissue grinder system (Fisher Scientific, Pittsburgh, PA) and then stored at -80 °C.

Cell Culture and Molecular Assays

TCID$_{50}$/CPE and DFA Assays

Starting viral titers were quantified by cell culture endpoint–dilution assays performed using Madin–Darby canine kidney (MDCK) cells and calculated using the Spearman–Kärber method (Armitage and Allen 1950) in units of $\log_{10}$ TCID$_{50}$/mL. Cell culture plates containing MDCK cells were grown and maintained using standard cell culture techniques.

Presence of viable virus in homogenates of murine lung tissue was qualitatively assessed by two concentration-dependent cell culture endpoint assays performed using MDCK cells. Cell culture plates containing MDCK cells were grown and maintained using standard cell culture techniques. Aliquots (1.0 mL) of lung homogenates were plated in serial 1:10 dilutions (in serum-free EMEM) from 10^{-1} to 10^{-4} in quadruplicate on confluent cell monolayers. The samples remained in contact with the monolayer for an hour's incubation before 1% BSA (bovine serum

albumin)–serum-free EMEM with trypsin was added. The plates were incubated for 5–6 days under 5% CO_2 at 37 ºC prior to visualization under the microscope for cytopathic effect (CPE) or fluorescent-labeled antibody evaluation. Test plates were read using a +/- system, in which + indicates that disruption of the monolayer was observed (virus present) and – shows that the monolayer remained confluent (no viable virus present).

Direct fluorescent antibody assay (DFA) was used to qualitatively determine influenza infection of the MDCK cell line using the D^3 Ultra DFA Respiratory Virus Screening and ID Kit (Diagnostic Hybrids Inc., Athens, OH) per manufacturer's instructions.

RNA Extraction and qRT-PCR

Ribonucleic acid (RNA) was extracted from samples using the QIAamp®MinElute®Virus Spin Kit following the manufacturer's protocol (Qiagen, USA). RNA amplification was performed using Invitrogen's Superscript III Platinum One-Step quantitative real-time polymerase chain reaction (qRT-PCR) kit (Invitrogen, USA). The qRT-PCR assay was run on the Roche LightCycler® 480 Real-Time PCR System (Roche Diagnostics). Assay conditions and reaction volumes were adopted from protocols previously described by the CDC (Centers for Disease Control and Prevention) (WHO, 2009). The cycle threshold (Ct) values from replicate runs were averaged for each time point and rounded to two decimal places. The CDC-recommended protocol threshold Ct value of 30 was used as the criterion for infection.

Histological Assay

Following fixation and routine processing, tissue sections were stained with hematoxylin and eosin (H&E) and reviewed under standard light microscopy.

Results

Results using the SMPS to measure the PSD from aerosolization of influenza virus indicated a

polydisperse aerosol comprising mostly fine and ultrafine particles (results not shown). The

power analysis revealed that a sample size of 15 mice per group (30 total) provides 87% power

to detect a 45% difference between the groups when the estimated rate of infection in the control

group is 50%. With 10 mice per group (20 total) there will be 80% power to detect a 55%

difference between the groups when the estimated rate of infection in the control group is 60%

(Table 1). Having an *n* of five was not shown on this table, but due to costs and overall mice

needed for all exposure ranges, we were advised that five mice per group would provide

statistically significant discrimination (personal communication, Elizabeth Lyden, M.S.,

Nebraska's Health Sciences Center, UNMC, Omaha, NE) (Hintze, 2004).

Table 1. Power analysis for the number of mice needed per treatment group to

achieve reliable detection of differences in infection rates.

Control proportion infected	Treated proportion infected	Detectable difference (Treated–Control)	*n* per group	Power
0.50	0.05	-0.45	15	86.97%
0.60	0.05	-0.55	10	79.58%

The virus was stable in the Collison nebulizer for up to 2 hrs in water as the aerosolization medium. Samples were taken up- and downstream throughout a 2-hr run and plated using the MDCK cell method to determine loss of viability; none was found (results not shown).

Two methods of plaque assay for infection of MDCK cells were used. The first involves the use of a stain to facilitate visualization of the viral plaques (direct fluorescent antibody assay [DFA]). The second was the $TCID_{50}$ assay followed by a crystal violet stain. Counts of plaques before and after staining indicated that the staining procedure did not alter the result of the assay but did make it much easier to visually assess the plaques (Appendixes C–D).

Intranasal Exposure
To select the optimal mouse strain for use with the influenza A/PR/8/34 (H1N1) (not mouse-adapted) strain used in this study, two inbred (BALB/c and C57BL) and one semi-outbred strain (CD-1) of mice were tested for susceptibility to infection by the virus.

Individual base weights were determined prior to exposure, and all mice were weighed daily at a uniform, scheduled time throughout the study. The average weights from surviving exposed mice at day seven were compared to the averages of control mice. All mice were euthanized by day seven post inoculation. Percent differences in weights are indicated in Table 2.

The non-mouse-adapted influenza virus produced obvious infection in all three strains of mouse used. PCR was completed on lung homogenates from one mouse in each exposure set; each of the mice from the virus-containing samples was positive (< 31 Ct (cycle threshold values)). As no difference in gross infectivity was indicated by weight loss and PCR was positive for all specimens, the less-expensive CD-1 mice were selected for further study.

Table 2. Percent weight loss versus controls following 30-μL intranasal
inoculation of influenza virus and seven-day incubation period.

Mouse Strain	%Weight Loss (Avg) after Inoculation with H1N1-A/PR-8 at a Dose of n TCID$_{50}$		
$n=$	4.74×10^7 TCID$_{50}$	4.74×10^6 TCID$_{50}$	0 (Controls)
CD57BL	28.2 (SD = 0.7)	28.0 (SD = 0.8)	0.1 (SD = 0.6)
BALB/c	26.2 (SD = 0.7)	19.0 (SD = 0.4)	0.6 (SD = 0.3)
CD-1	25.8 (SD = 0.6)	23.5 (SD = 1.5)	0.2 (SD = 0.9)

SD = Standard Deviation

Aerosol Exposure (1.58×10^6 TCID$_{50}$/mL)
A preliminary study was conducted to establish a baseline dose of virus capable of causing infection following aerosolization. The working stock of influenza virus was diluted 1:30 in endotoxin-free water (Sigma) and delivered into the Collison nebulizer at 1.58×10^6 TCID$_{50}$/mL. Four sets of three CD-1 mice were emplaced in polycarbonate restraints, installed into the CATS with the filter holder empty, and exposed to aerosolized virus at exposure times of 2, 6, 20 and 60 min. Two mice were used as unexposed controls. All of the mice survived to day 7, when they were euthanized and necropsied, and their lung tissue was examined by three different assays.

At all four exposure time points, mouse lung tissues gave positive results from the qRT-PCR assay, for which a positive value was defined to be < 31 Ct. DFA and CPE assays on the lung

tissue were also all positive (Table 3). There was a direct correlation between dose received (for

convenience reckoned as *Ct* values (product of concentration and exposure time)), with lower

PCR Ct values resulting from prolonged exposure. The mean Ct value for control mice was 37,

which we defined to be a negative response. Values of $37 > Ct > 30$ were considered

indeterminate. Weight losses again showed proportionality to dose delivered. The results

demonstrated that the influenza virus remained viable and capable of causing infection in CD-1

mice when aerosolized under test conditions.

Table 3. Results of three assays (PCR, DFA and CPE) from the homogenates of CD-1

murine lung tissue exposed to an aerosol generated from 1.58×10^6 TCID$_{50}$/mL (1:30

dilution) of influenza virus over four different exposure times are indicated in parentheses:

Pos = positive, Ct < 31; Ind = indeterminate, $37 \geq Ct \geq 31$; and Neg = negative, Ct > 37.

Concentration (TCID$_{50}$/mL)	Exposure Time (min)	Presented Dose (TCID$_{50}$)	Weight Gain (% ± SD)[‡]	PCR Ct	DFA	CPE
1.58×10^6	2	120	-2.0 ± 0.2	Pos (23)	Pos	Pos
1.58×10^6	6	360	-8.4 ± 0.2*	Pos (18)	Pos	Pos
1.58×10^6	20	1200	-17.3 ± 0.9	Pos (16)	Pos	Pos
1.58×10^6	60	3600	-14.7 ± 1.8	Pos (17)	Pos	Pos
1.58×10^6	Control	0	+6.9 ± 0.2	Neg (37)	Neg	Neg

[‡] Weight change percentage is the average of all three mice on day seven post exposure.

*1/3 mice died of unrelated cause.

Aerosol Exposure (1.58x10^5 TCID$_{50}$/mL)

Because exposure to the 1:30 dilution of aerosolized virus resulted in massive but graduated

infection of all tested mice, a greater dilution of the working stock was delivered in an effort to

identify a threshold infective dose. The dilution was increased tenfold (to 1:300, resulting in

delivery of a 1.58x10^5 TCID$_{50}$/mL dispersion from the nebulizer and an overlap (as *Ct* products)

of the two smaller doses from the 1:30 dilutions) and the initial aerosol exposure sequence was

repeated. Three mice per time point were assayed by qRT-PCR. Variation in Ct values was

observed in the 2-min exposure group, one mouse being clearly positive as reflected by Ct values

and the other two mice falling within the indeterminate range (Table 4). All mice in the 6-, 20-

and 60-min time points were positive (< 31 Ct) with minimal variation in Ct values. All control

mice were negative (Ct values > 37).

Table 4. PCR Ct values from the homogenates of CD-1 murine lung tissue exposed to

bioaerosol generated from a 1.58x10^5 TCID$_{50}$/mL dilution of influenza virus over four

different exposure times are indicated in parentheses: Pos = positive, Ct < 31; Ind =

indeterminate, $37 \geq$ Ct ≥ 31; and Neg = negative, Ct > 37.

Exposure Time (min)	Presented Dose (TCID$_{50}$)	Group 1	Group 2	Group 3
2	12	Ind (36)	Pos (19)	Ind (36)
6	36	Pos (20)	Pos (21)	Pos (14)
20	120	Pos (18)	Pos (19)	Pos (20)
60	360	Pos (17)	Pos (15)	Pos (18)
Control	0	Neg	Neg	Neg

TCID$_{50}$ assays were performed on mice from Group 1 at each time point. One mouse lung homogenate in Group 1 that was indeterminate by qRT-PCR (36 Ct) was negative by TCID$_{50}$ assay. All other lung homogenates tested positive by both methods, except the controls, which were all negative.

Aerosol Exposure (4.7 x 10^4 TCID$_{50}$/mL)
Although weight loss by the mice appeared to have reached baseline at the dose delivered in 6 min at 1:300 dilution, Ct results from the aerosol challenge at 1:300 dilution show that all the mice exposed for 6 min or more received an infectious dose. In an effort to better define the threshold at which viral infection occurs the stock solution was further diluted to 4.7x10^4 TCID$_{50}$/mL (1:1000), the exposure times were reduced, the number of mice per time group was increased to five, and two additional time points were added to increase the range and dose of aerosol exposure. Results of this test are shown in Table 5.

Table 5. PCR Ct values from homogenates of CD-1 murine lung tissue exposed to aerosol generated from a 4.74 x 10^4 TCID$_{50}$/mL dilution of influenza virus over five different exposure times are indicated in parentheses: X = mouse death; Pos = positive, Ct < 31; Ind = indeterminate, $37 \geq Ct \geq 31$; and Neg = negative, Ct > 37.

Exposure Time (min)	Presented Dose (TCID$_{50}$)	Group 1	Group 2	Group 3	Group 4	Group 5
3	6	Neg	Neg	Neg	Neg	Neg
6	12	Neg	Neg	Neg	Neg	Pos (22)
9	18	Ind (33)	X	Neg	Ind (37)	Pos (20)
12	24	Ind (31)	Neg	Neg	Pos (23)	Neg
18	36	Ind (33)	Ind (33)	Pos (27)	Ind (37)	Neg

At the 3-min exposure time, no mice were positive for influenza virus as determined by Ct value. In all four of the longer-exposure groups a single mouse displayed a positive Ct value. A trend may be suggested by the pattern of indeterminate values, but the quantitative Ct values show an equally unconvincing opposite trend. All of the lung homogenates were tested by virus cell culture assay for $TCID_{50}$ and DFA. For homogenates whose Ct value is < 31, both $TCID_{50}$ and DFA were positive.

Histological Assay

Influenza-infected lungs showed lobular pneumonia with interbronchial inflammation and focal chronic inflammatory cell infiltration with a few neutrophils and some interstitial thickening. Figure 9 compares infiltrates in infected tissue to uninfected tissue.
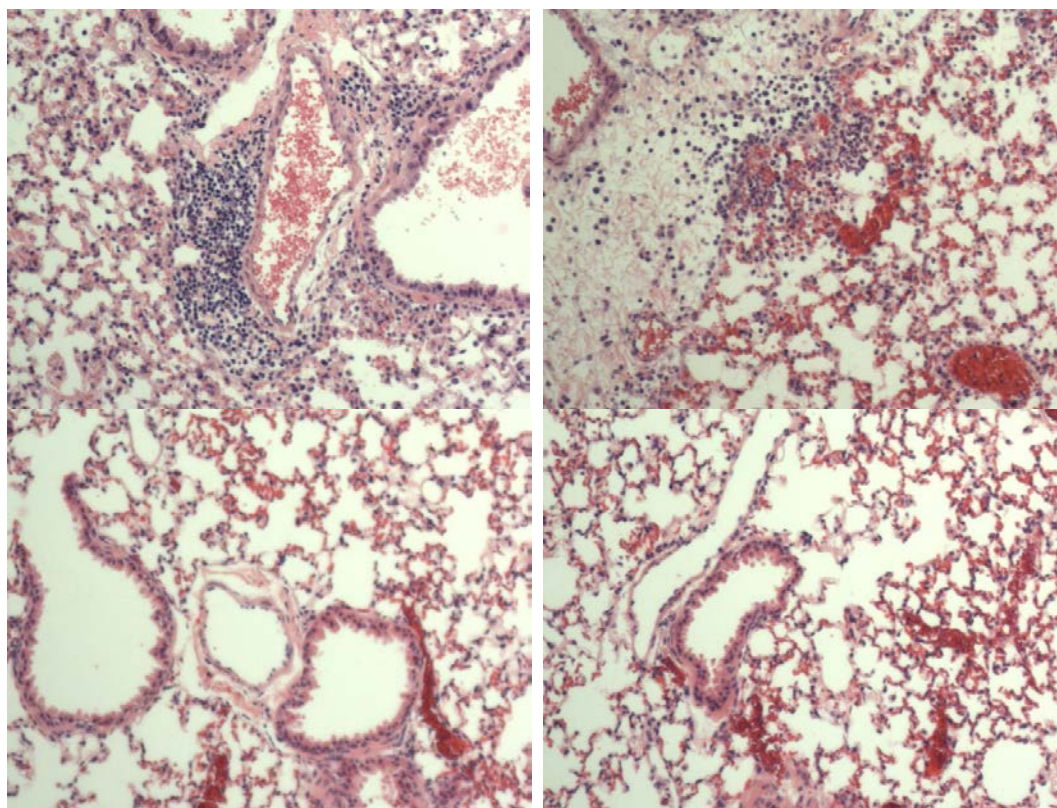
Figure 9. Top: Mouse lung image after exposure to aerosolized virus; H&E staining technique.

Bottom: Mouse lung image after exposure to sterile aerosols (no virus noted).

Discussion

Influenza A/PR/8/34 (H1N1) virus is a spherical, small (80–120 nm), enveloped RNA virus of the family Orthomyxoviridae. It was found to be infectious to general mouse strains (BALB-c, C57Bl and CD-1 mice) and able to withstand aerosolization for 2 hrs in water. As any additional buffer solutions would coat the virus particles and make the droplets larger, affecting our penetration studies, it was necessary to find a minimal medium for aerosolization.

Transmission of Influenza

It is accepted that influenza may be contracted through at least four methods: (1) contact, (2) inhalation, (3) inspiration and (4) direct spray, but the predominant route is still uncertain (Jones and Adida, 2011). Jones and Adida (2011) have defined the difference between inhalation and inspiration based on size of the particle and where it deposits in the respiratory tract: inhalation is defined as respiring particles 10 µm and smaller in diameter, which deposit throughout the upper and lower respiratory tract. In contrast, inspiration is defined as respiring particles 10–100 µm in diameter, which deposit in the upper respiratory tract. The only route of infection examined during this study was inhalation of droplet nuclei through nasal passageways and we did not examine other organs for presence of virus; that work has been done by others (Lu et al., 1999). Results should be expected to differ if other mucosal surfaces had been dosed with the same viral aerosols. Research by van Riel et al. (2007) has also found that, based on viral cell specificity, the subtype of influenza virus may determine where in the respiratory tract deposition occurs, affecting the virus' host preference, pathogenesis and treatment methods. Our study sought only to determine the existence and scale of a measurable threshold aerosol infective dose in this

animal model and to set parameters—such as the mouse restraints in the experiment—that limit other exposure.

Although this study demonstrated infectivity of the aerosol, its residence time as dispersed fine particles was short—hundreds of milliseconds from nozzle to nose—and viruses are known to spontaneously lose viability, so the importance of such bioaerosols as an environmental component remains uncertain. However, the experiment accurately simulates exposure to a direct spray such as a cough, which can accordingly be concluded to be a mechanism for immediate transmission of this virus.

Although considerable support has been documented supporting the transmissibility of influenza A by inhalation routes, few studies to date have utilized a mouse model to investigate susceptibility to and pathogenicity of aerosol exposures. The lack of aerobiology studies results from several factors including the need for specialized equipment to generate and monitor bioaerosols, the technical difficulty involved, inconsistency in techniques and the considerable cost and time associated with animal research. As a consequence, the most commonly described method of infecting mice with influenza virus is by installation of fluid into the nasal passages. The purpose of this study was to identify a susceptible small animal and to experimentally determine its suitability to function as a quantitative detector of a consistent, inhaled, infective dose of pathogenic aerosol—to serve as the detector for the complementary CATS.

Green and Kass (1964) conducted studies on the clearance of inhaled microbial aerosols from the murine respiratory tract. Shulman and Kilbourne (1963) studied mouse-to-mouse transmissibility of influenza virus. They both note that a factor complicating viral research in animal models is that a virus may be present in a host without causing disease. This may be due to such

restrictions as absence of appropriate receptors on certain cell types (e.g., tissue tropism) or of intracellular processes required to generate infectious progeny viruses or induce cytolytic effects. Differences in viral receptors have been documented for respiratory epithelial cells based on location in either the pharynx or peripheral lung (van Riel et al., 2007; 2010). In addition, either the organism or host cell may mount an immune response or generate intracellular molecules that disrupt the viral effects. Differences may appear at either the cellular or tissue level or among susceptible hosts depending upon the method of infection, especially in regard to aerosol exposures (Phalen et al., 2008). Our current study examined these parameters related to efficient infection versus gross infection of mice using aerosolized influenza virus.

It should be noted that an exact dose of virus needed to cause respiratory influenza infection post filtration has not been quantified. What we have done is establish a model that now can be used not only with influenza, but with any airborne pathogen of interest to determine respiratory dose of infection. This has broad-reaching applications in the realm of respiratory infection control such as respiratory protection devices and vaccine development.

Measurements of Response
We considered three different thresholds to determine infectivity: clinical response, based on weight change; cytopathic effect (CPE/ $TCID_{50}$), based on cellular response in MDCK cells and qRT-PCR data; and immune response, measurement of which was beyond the scope of this project. We determined two different MID_{50} values, one based on the clinical response and the other based on the combined results of the CPE/ $TCID_{50}$ assays. The difference in the two values can be interpreted as revealing a higher threshold for a clinical response than for a cellular response or a threshold for an overwhelming dose that defeats the immune response. The

threshold for an immune response—which is not necessarily accompanied by a cellular or clinical response—is certainly lower, by some amount we were unable to estimate.

When discussing infection or detection endpoints, it is important to determine which endpoint is meant, as different fields of study may have a different definition of an endpoint. For example, a healthcare provider may not be concerned with the qRT-PCR data of a patient that shows virus to have been present in small quantities, but concern may grow if a cellular-level response is noted, meaning the patient is either asymptomatic or pre-symptomatic and may possibly be spreading the virus. A healthcare provider would be much more interested in data showing clinical changes in the patient such as marked weight loss, fever or body aches. But for our work measuring filter penetration of infectious agents, the reproducible threshold dose producing a positive Ct by qRT-PCR provides the quantitative endpoint needed to evaluate the extent of protection (attenuation of infectivity) afforded by the RPE device being tested, calculated as the ratio of challenges applied at which the received dose equals the MID_{50} with and without the RPE article in place.

Infectivity/ clinical symptoms
The only clinical response evaluated was weight change. We did not monitor other common signs/symptoms of infection such as fever, body posture and loss of appetite. This is considered the least sensitive assay for detection of the virus, as by the time clinical effects are noticed, the animal is probably highly infected and shedding loads of the virus and has lost cells damaged by the viral release.

Our results showed significant variation in morbidity and mortality among the mice exposed to aerosolized influenza virus. This appears to have been due to individual susceptibility of the mice, because variability in the uniformity of the aerosol delivered was found not to be signif-

icant when each of the ports was analyzed. In addition, significant differences were noted when mice were exposed over times ranging from 6–18 min with minimal or no morbidity when a low quantity of virus was sprayed over an extended period of time. For example, in Table 4 at the lowest exposure time one of the three mice was positive for infection whereas in the lowest-dose experiment (Table 5) one mouse was positive following only 6 min of exposure. In contrast, the larger doses of virus over even short exposure times caused greater losses in the weight of those mice. What we believe is happening is that the mice who received the smaller doses over a longer time period were able to process and clear a significant fraction of the virus received, as opposed to the mice who were hit with a large dose over a short time and were unable to resist the viral challenge. Additionally, the hardiness of immune response to influenza varies among the mice, resulting in different levels of susceptibility, displayed as random variability within the population.

As do many viruses, influenza produces a significant number of defective particles incapable of causing infection (Huang, 1973; Pathak and Nagy, 2009). This is further demonstrated by the wide variation—ranging from hundreds to thousands—in reported gene copy (total virions)-to-dose (in $TCID_{50}$) (infectious virion fraction) ratio (Yang et al., 2011). Sidorenko and Reichl (2004) developed a mathematical model describing the complete life cycle of influenza A in animal cells. This model, based on a multiplicity of infection (MOI) of 10 virions/cell, suggests that influenza replicates within 5 hrs post infection and produces up to 8,000 progeny virions before cell death occurs. Perrott et al. (2009) reported a detection level for influenza A (H1N1) of 1 $TCID_{50}$ using qRT-PCR and 0.1 $TCID_{50}$ using nested qRT-PCR. If one accepts that a direct correlation may not always exist between a method that detects viable organisms and one based on viral genomes, our system showed excellent correlation between classical virology methods,

morphology based on histologic examination, clinical features and molecular quantification by qRT-PCR.

Influenza infection in mice has been monitored by several different parameters including mean time to death, lung weight and change in body weight (Sidwell and Smee, 2000; Raut et al., 1975; Gillim-Ross, 2008). However, these indicators are difficult to interpret when the infectivity and challenge dose of the virus do not clinically manifest an illness (morbidity or mortality). There-fore we compared qRT-PCR data with $TCID_{50}$ results to narrow the variability. Virus replica-tion in lung tissue is considered the most informative endpoint for efficacy studies—even modest changes in virus load can have a large impact on survivability (Haga and Horimoto, 2010).

Detection Level of the $TCID_{50}$ Assay
We used the CPE/$TCID_{50}$ as the cytopathic assay detection method. This assay shows a cellular response to viral infection. We consider this assay more sensitive than the mouse's exhibiting clinical symptoms, but the assay method itself is still not as sensitive as qRT-PCR (Freeman, 1999).

The detection level of a $TCID_{50}$ assay is defined as the lowest dilution tested for which at least one positive well (displaying CPE) is observed among a given number of replicates. Many factors can influence the detection level of the $TCID_{50}$ assay, as it is a function of the number of replicates tested at each dilution, the total volume in each well of the assay plate, the volume of the original sample and the lowest dilution tested. The detection level is calculated using a Kärber formula (see Appendix) and using one positive well out of a given number of replicates (typically four replicates per dilution), and all other variables in the Kärber formula reflect the actual parameters used in the given $TCID_{50}$ assay. The titer is then translated into total $TCID_{50}$

units by taking into account the total volume of the original sample in the impinger and, if only a portion of the effluent air is sampled, by proportionally adjusting for the flow rate—here by multiplying by 7.08 to scale from the actual sampling flow rate of 12 LPM to the NIOSH-standard flow rate of 85 LPM passing through the air filtration product.

Animal models

It is important to note that this strain of influenza was not mouse adapted in our lab or any other. This shows that the mice are susceptible to influenza in its original form as an aerosol. Considering this as a mouse model for human infection, we might be able to infer that human susceptibility would be just as easy from a novel strain of influenza not previously in contact with human cells via the aerosol route.

Assays of post-sacrifice tissue samples from the mice were uniformly positive in the 1:30 dilution series. In contrast with the data shown in Figure 10, in the 1:300 dilution series the 2-min exposure (12 $TCID_{50}$ dose) group contained subjects that were not unequivocally positive for infection, both by Ct (2 of 3) and by CPE (1 of 3). One-way ANOVA and a two-tailed t-test did not find any statistical differences between the change in the mouse's weight and the PCR data; however, a more-precise threshold value and statistical significance of this difference can be expected when the number of mice (n) in each exposure group is increased. Likewise, the two sets of subjects that shared Ct products (2 min x 1:30 and 20 min x 1:300, and 6 min x 1:30 and 60 min x 1:300) appear to show increased sensitivity with increasing aerosol concentration, which could be taken to imply that an acute exposure leads to greater infectivity than the same dose experienced more gradually. Although this interpretation is intuitively reasonable, the volume of data supporting it is too limited to justify such a conclusion.
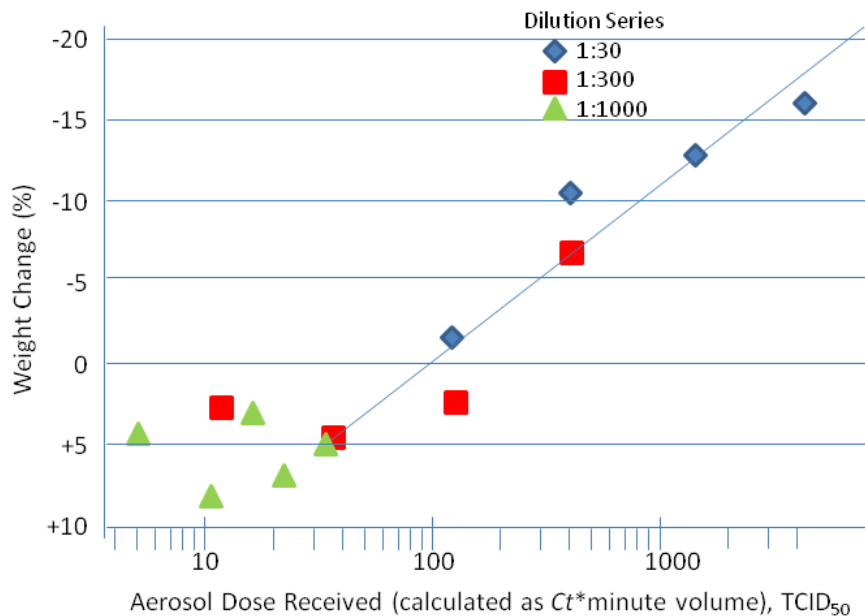
Figure 10. Average weight change for mouse exposure groups over three

different received aerosol doses. Plot shows overlap between doses

received and change in weight, leading to the determination of an MID_{50}.

Estimate of infective dose

After selecting both a suitable organism (influenza virus A/PR/8/34 (H1N1), not mouse adapted)

and a susceptible animal model (CD-1 strain) we performed three sets of aerosolized-dose-

exposure experiments. Weight gain or loss, survival status and necropsy data were obtained for

each participating mouse. Post-mortem assays included CPE, DFA and $TCID_{50}$. The first set,

comprising exposures for $t = 2$, 6, 20 and 60 min to an aerosol generated from a 1:30 dilution of

the viral stock, resulted in gross infection of all of the mice but revealed a trend of symptomatic

response to dose. A second series was conducted delivering 1:300 dilution of the viral stock, in

which two Ct values (6 min in the 1:30 series and the 60 min in the 1:300 series,$(Ct = 6/30 =$

60/300) and 2 min in the 1:30 set and 20 min in the 1:300 set ($Ct = 2/30 = 20/300$) were repeated

to ensure data overlap. The bioaerosol dose received is calculated as follows:

D_p (presented dose) = viral titer*dilution factor*VSF*r_a*V_a*t

Where r_a is the respiration rate and V_a is the tidal volume, respectively, of the CD-1 mouse,

which respective values are reported (Fairchild, 1972) to be 261 respirations/min and 0.16 mL_A

(mL of air). Thus, a mouse exposed for 2 min to a 300:1 dilution of a suspension containing

4.74×10^7 $TCID_{50}$/mL inhales a dose of

$$D_p = 4.74 \times 10^7 \ TCID_{50}/mL * 1/300 * 9 \times 10^{-7} \ mL/mL_A * 261 \ resp/min * 0.16 \ mL_A/resp * 2 \ min$$

$$= 12 \ TCID_{50}$$

Owing to logistical factors in the ABSL-3 facility the PSD was not measured during exposures.

However, Stone (2010; Stone et al. 2012) measured bioaerosol particles in the range

100~500 nm for a slightly smaller virus (MS2 coli phage) in the same apparatus. The absorbed

dose was likely slightly smaller than the presented dose because deposition of inspired particles

in this size range is incomplete and size dependent (Clay and Clarke, 1987; Heyder, 2004; Stuart,

1973). A plot of weight loss vs. calculated inhaled dose (Figure 10) was fitted to a straight line,

which intersects the mean weight change of the control group at approximately 40 $TCID_{50}$. A

third series of exposures was performed to a 1:1000 dilution, intended to improve definition of

the threshold dose for weight loss; however, the results were equivocal, likely because the

delivery was gradual enough that the mice developed an immune response that was able to

manage the challenge and/or the n of five was too small to average out what we presume to have

been idiosyncrasies among the subjects.

Our results showed that qRT-PCR was more sensitive or that an excess of genome was present in comparison with the number of infectious virions as determined by $TCID_{50}$ and DFA assays. As the gold standard (Schrauwen et al., 2011) for determining the MOI has been $TCID_{50}$ and quantification of virus in mice exposed to influenza aerosols by qRT-PCR has not been previously reported, additional confirmatory studies were needed. We chose seven days as the terminal point for our study based on symptomatology in humans, in whom virus production peaks approximately 48 hours post infection and few virus particles are shed after day six (Taubenberger and Morens, 2008). Our results showed the delivered aerosol MID_{50} to be at least 12 $TCID_{50}$ as determined by qRT-PCR Ct value and significantly less that 40 $TCID_{50}$ as determined by obvious clinical response. However the sample size must be expanded in the future to achieve greater resolution and statistical significance. In addition, future studies will utilize the influenza virus A (H1N1) pdm strain to determine variation in MID_{50} between the two strains.

Future Directions
Significance of project

Work presented herein validates aerosolization of one viral pathogen and delivery by a pure respiratory pathway into one susceptible murine host as a novel technique for assaying infectivity by a challenging bioaerosol. This project is a starting point for quantitative infectivity studies using the CATS that may advance the state of understanding of mechanisms of respiratory infection by viruses, bacteria or other organisms and inform efforts to combat their spread and clinical intensity. Neumann et al. (1999) are using a new reverse-genetics system to create influenza viruses entirely from cloned cDNAs; they have successfully proven infectivity in cell lines, but to quantitatively characterize their new creations, an infection assay system will

be needed, and the CATS with an appropriate animal model and baseline for MID_{50} would be useful to obtain those data.

The data and methods presented herein contribute to a fundamental basis for refining studies of aerosol delivery of particles into animal models for study of a variety of clinical subjects, such as infectious doses and vaccine delivery. Further work will be needed to more precisely define the median infective dose (MID_{50}) of influenza A/PR/8/34 (H1N1) in the CD-1 mouse, and to elucidate the effect of bioaerosol aging and dose rate on infectivity. The work of Denkers et al. (2010), studying chronic wasting disease in a mouse model is an example of an infectivity system that could better be examined by this technique.

In our experiments temperature and RH were kept "constant" as room temperature and humidity, although the CATS has the capability to vary both (Stone, 2010). Variation of either or both can be expected to produce different results for virus survivability, infectivity, and possibly even filter penetration. It is well documented that many viruses spread best in cold, dry air; holding some environmental conditions constant (e.g., temperature, pressure, humidity, host status, stressing factors, coadministered agents) and varying others will pinpoint factors or combinations of factors that influence infectivity, which might suggest measures to suppress the spread of or ameliorate the course of infection. Vlodavets and Dmitriyeva (1966) showed that viruses lose viability faster in humid air, particularly non-enveloped viruses such as influenza A and adenovirus. Our procedure used a constant, short time from aerosolization to exposure. Extending the pathlength traveled by the aerosol or detaining it in a ballast will allow systematic variation under controlled conditions of the age of the aerosol at exposure, from which a precise description of the rate of attenuation of infectivity can be determined.

The intended application of the aerosol influenza animal model described here is the assessment of the clinical effect of respiratory protection devices incorporating antimicrobial treatments. Various approaches have been proposed to increase the effectiveness of respiratory filtering media including the addition of bioactive media. Although materials such as silver nanoparticles (Lala et al. 2007), copper oxide (Borkow et al. 2010), iodinated compounds (Heimbuch and Wander 2006) and others (Cecchini et al. 2004) have shown biocidal potential, only the iodine vector has been proposed (Lee et al. 2009) to operate by a noncontact mechanism. Additional studies will focus on evaluating such new technologies (e.g., photogenerated singlet oxygen) and, after replacement of the filter holder with a larger enclosure able to collect aerosols behind RPE worn by an articulated headform (Bergman et al., 2012), on quantifying the effect on protectivity of seal leakage and on optimizing the particle removal efficiency of respiratory protective equipment to measure net protectivity.

McClellan (2009) has performed numerous studies with mice and mathematical modeling examining location of deposition in the respiratory tract as a function of aerosol particle size, using *F. tularensis* as a model organism, and Roy (2003) has studied deposition of ricin aerosols. These studies could be compared more easily if they had been performed in a uniform aerosolization device such as CATS.

In addition to being used to unify aerosol data, the CATS can be fed by a virtual classifier (right angle jet) to deliver particles of discrete sizes, ranging from ultrafines (<100 nm) to fine (<1000 nm or less) and larger particles. Because the goal was to evaluate particles penetrating a filter, we used predominately fine particles near the MPPS as part of our study, but the CATS allows for particles of a range of sizes and compositions to be used and classified (Stone et al., 2012).

Although we performed nose-only studies, the CATS can be employed to study other respiratory routes, although different animal models may be needed to compare nose to mouth breathing. Other mucosal surfaces, such as ocular infection may be of interest to the medical or biowarfare mitigation communities. Although we studied only influenza A virus in this portion of the project, other infective particles should be considered. Studies involving co-delivered materials would be of interest especially concerning areas of public health, bioterrorism and biowarfare zones.

REFERENCES

1. Ali, M.; Harnish, D. et al. Accelerated Attenuation of Viability of Bioaerosols by Acquired Oxidants. *Proceedings of the 30th Annual Conference, presented by the American Association for Aerosol Research*, Orlando, FL, October 3-7, 2011.
2. Andrewes, C., Laidlaw, P. et al. The Susceptibility of Mice to the Viruses of Human and Swine Influenza. *Lancet,* 1934, *224*, 859–862.
3. Armitage, P., Allen, I. Methods of estimating the LD_{50} in quantal response data. *J Hyg. (Lond).* 1950, *48*(3), 298–322.
4. Bailar, J.; Burke, D. et al. Reusability of facemasks during an influenza pandemic. Institute of Medicine, National Academies Press: Washington, DC, 2006.
5. Beigel, J.; Bray, M. Current and future antiviral therapy of severe seasonal and avian influenza. *Antiviral Res*. 2008, *78*, 91–102.
6. *Biosafety in Microbiological and Biomedical Laboratories* (BMBL), 5th Edition. U.S. Department of Health and Human Services, 2009.
7. Brankston, G.; Gitterman, L. et al. Transmission of Influenza A in Human Beings. *Lancet Infect. Dis*. 2007, *7*, 257–265.
8. Bross, I. Estimates of the LD_{50}: A Critique, *Biometrics*, 1950, *6*, 413–23.
9. CDC Seasonal Influenza (Flu) Fact Sheet 2011- Flu Season 2012. http://www.cdc.gov/flu/about/season/index.htm.
10. Center for Food Security and Public Health (CFSPH). Iowa State University, Ames, IA. http://www.cfsph.iastate.edu/Factsheets/pdfs/tularemia.pdf 2007.
11. Centers for Disease Control. Avian Influenza U.S. Resources. 2012a. http://www.cdc.gov/niosh/topics/avianflu/usresources.html
12. Chen, W.; KuoLee, R.; Austin, J.; Shen, H.; Conlan,J. Low dose aerosol infection of mice with virulent type A *Francisella tularensis* induces severe thymus atrophy and $CD4^+$ $CD8^+$ thymocyte depletion. *Microb. Pathog*. 2005, *39*, 189-196.
13. Chen, W.; KuoLee, R.; Shen, H.; Conlan,J. Susceptibility of immunodeficient mice to aerosol and systemic infection with virulent strains of *Francisella tularensis*. *Microb. Pathog*. 2004, *36*, 311-318.
14. Cheng, Y. and Moss, O. Inhalation Exposure Systems. Toxicology Mechanisms and Methods. 1995, *5*, 161-197.
15. Clay, M.; Clarke S. Effect of nebulised aerosol size on lung deposition in patients with mild asthma. *Thorax.* 1987, *42*, 190–194.
16. Conlan, J.; Chen, W.; Shen, H.; Webb, A.; KuoLee, R. Experimental tularemia in mice challenged by aerosol or intradermally with virulent strains of *Francisella tularensis*: bacteriologic and histopathologic studies. *Microb. Pathog*. 2003, *34*, 239-248.
17. Denkers N.; Seelig D. et al. Aerosol and nasal transmission of chronic wasting disease in cervidized mice. *J. Gen. Virol*. 2010, *91*, 1651–1658.
18. Drew, R. and Laskin, S. Environmental Inhalation Chambers. Methods of animal experimentation. New York; Academic Press. 1973, *4*, 1-41.
19. Eigelsbach, H. and McGann, V. Genus *Francisella*. In Bergey's Manual of Systematic Bacteriology; Krieg, N.; Holt, J. Eds.; Williams and Wilkins: Baltimore, MD, 1984, Volume 1, 394-399.
20. Fairchild, G. Measurement of Respiratory Volume for Virus Retention Studies in Mice. *Appl. Microbiol.* 1972, *24*(5), 812-818.

21. Finney, D. *Statistical Methods in Biological Assay, 2nd ed*. Griffin, London, England. pp. 524–530, 1964.

22. Franz, D.; Jahrling, P. et al. Clinical Recognition and Management of Patients Exposed to Biological Warfare Agents. *J Am. Med. Assoc*. 1997, *5*, 399-411.

23. Freeman, W.; Walker, S. et al. Quantitative RT-PCR: Pitfalls and Potential. *Biotechniques*. 1999. *26*, 112-125.

24. Gautret, P.; Botelho-Nevers, E. et al. The spread of vaccine-preventable diseases by international travelers: A public-health concern. *Clinical Microbiology and Infection*. 2012. DOI: 10.1111/j.1469-0691.2012.03940.x

25. Gillim-Ross, L., Santos, C., et al. Avian Influenza H6 Viruses Productively Infect and Cause Illness in Mice and Ferrets. *J. Virol*. 2008, *82*, 10854–10863.

26. Green, G.; Kass, E. Factors Influencing the Clearance of Bacteria by the Lung. *J. Clin. Invest*. 1964, *43*, 769–776.

27. Gubareva, L.; McCullers, J. et al. Characterization of Influenza A/HongKong/156/97 (H5N1) Virus in a Mouse Model and Protective Effect of Zanamivir on H5N1 Infection in Mice. *J. Infect. Dis.* 1998, *178*(6), 1592–1596.

28. Haga, T., Horimoto, T. Animal Models to Study Influenza Virus Pathogenesis and Control. *Open Antimicrob. Agents J*. 2010, *2*, 15–21.

29. Hayden, F. Prevention and Treatment of Influenza in Immunocompromised Patients. *Am. J. Med*. 1997, *102*, 55–60.

30. Heyder, J. Deposition of Inhaled Particles in the Human Respiratory Tract and Consequences for Regional Targeting in Respiratory Drug Delivery. *Proc. Am. Thorac. Soc.* 2004, *1*(4), 315–320.

31. Hintze, J. NCSS and PASS. Number Cruncher Statistical Systems. Kaysville, Utah. 2004. www.ncss.com.

32. Hogan, C.; Kettleson, E. Sampling methodologies and dosage assessment techniques for submicrometre and ultrafine virus aerosol particles. *J. Appl. Micro*. 2005, *99*, 1422-1434.

33. Huang, A. Defective Interfering Viruses. *Annu. Rev. Microbiol*. 1973, *27*(1): 101–118.

34. Iwen, P. University of Nebraska Public Health Laboratory, Omaha, NE, 2008.

35. Jaeger, R., Shami, S. G. et al. Directed-Flow Aerosol Inhalation Exposure Systems: Applications to Pathogens and Highly Toxic Agents. Inhalation Toxicology. H. Salem and S. A. Katz. Boca Raton, CRC Press. 2006, 73-90.

36. Jerrells, T.; Pavlik, J. et al. Association of chronic alcohol consumption and increased susceptibility to and pathogenic effects of pulmonary infection with respiratory syncytial virus in mice *Alcohol.* 2007, *41*(5), 357–369.

37. Jhung, M.; Swerdlow, D. et al. Epidemiology of 2009 Pandemic Influenza A (H1N1) in the United States. *Clin. Infect. Dis.* 2011, *52*(suppl 1), S13–S26.

38. Jones, R.; Adida, E. Influenza Risk and Predominate Exposure Route: Uncertainty Analysis. *Risk Analysis*. 2011, 31(10), 1622–1631.

39. Lee, V. Reflection and Reaction—Transmission of Influenza A in Human Beings. *Lancet Infect. Dis*. 2007, *7*, 760–761.

40. Lemieux, C.; Brankston, G. Questioning Aerosol Transmission of Influenza. *Emerging Infect. Dis.* 2007, *13*, 173–174.

41. Lu, X.; Tumpey, T. et al. A Mouse Model for the Evaluation of Pathogenesis and Immunity to Influenza A (H5N1) Viruses Isolated from Humans. *J Virol*. 1999, *73*, 5903–5911.

42. Lyden, E. University of Nebraska Public Health Laboratory, Omaha, NE, 2009.

43. MacFarland, H. Designs and Operational Characteristics of Inhalation Exposure Equipment — A Review. Fund. Appl. Toxicol. 1983, *3*, 603–613.

44. Moyer, E.S.; Stevens, G.A. "Worst case" aerosol testing parameters: II. Efficiency dependence of commercial respirator filters on humidity pretreatment. *Am. Ind. Hyg. Assoc. J.*, 1989, *50*, 265–270

45. Neumann, G. Watanabe, T. et al. Generation of influenza A viruses entirely from cloned cDNAs. *Proc. Natl. Acad. Sci., USA*. 1999, *96*, 9345–9350.

46. Ng W.; Wong V. et al. Prevention and Treatment of Influenza with Hyperimmune Bovine Colostrum Antibody. *PLoS ONE*. 2010, *5*(10), e13622.doi:10.1371/journal.pone.0013622

47. Oxford, J. Influenza A pandemics of the 20th century with special reference to 1918: virology, pathology and epidemiology. *Rev. Med. Virol*. 2000, *10*, 119–133.

48. Pathak, K., Nagy, P. Defective Interfering RNAs: Foes of Viruses and Friends of Virologists. *Viruses.* 2009, *1*(3), 895–919.

49. Perrott, P., Smith, G., Ristovski, Z., Harding, R., Hargreaves, M. Nested real-time PCR assay has an increased sensitivity suitable for detection of viruses in aerosol studies. *J. Appl. Microbiol.* 2009, *106*(5), 1438–1447.

50. Phalen, R., Oldham, M. et al. The relevance of animal models for aerosol studies. *J. Aerosol Med. Pulm. Drug Delivery*. 2008, *21*, 113–124.

51. Raut, S.; Hurd, J. et al. The Pathogenesis of Infections of the Mouse Caused by Virulent and Avirulent Variants of an Influenza Virus. *J. Med. Microbiol.* 1975, *8*, 127–136.

52. Relman, D. Bioterrorism-Preparing to fight the next war. *N Engl J Med*. 2006, *354*, 113-115.

53. Schrauwen, E.; Herfst, S. et al. Possible Increased Pathogenicity of Pandemic (H1N1) 2009 Infl uenza Virus upon Reassortment. *Emerging Infect. Dis.* 2011, *17*(*2*), 200–208.

54. Schulman, J.; Kilbourne, E. Experimental Transmission of Influenza Virus Infection in Mice. I. The Period of Transmissibility. *J Exp Med*. 1963,*118*, 257–266.

55. Sidorenko, Y., Reichl, U. Structured model of influenza virus replication in MDCK cells. *Biotech. Bioeng.* 2004, *88*(1), 1–14.

56. Sidwell, R.; Smee, D. Experimental disease models of influenza virus infections: recent developments. *Drug Discovery Today: Dis. Models.* 2004, *1*(1), 57–63.

57. Sidwell, R.; Smee, D. In vitro and in vivo assay systems for study of influenza virus inhibitors. *Antiviral Res.* 2000, *48*, 1–16.

58. Smee, D.; Bailey, K. et al. Treatment of influenza A (H1N1) virus infections in mice and ferrets with cyanovirin-N. *Antiviral Res*. 2008, *80*, 266–271.

59. Stone, B. Consistency and Reproducibility of Bioaerosol Delivery for Infectivity Studies on Mice. M.S. Thesis, University of Florida, Gainesville, FL, 2010.

60. Stone, B. Consistency and Reproducibility of Bioaerosol Delivery for Infectivity Studies on Mice. M.S. Thesis, University of Florida, Gainesville, FL, 2010.

61. Stone, B.; Heimbuch, B. et al., Design, Construction and Validation of a Nose-Only Inhalation Exposure System to Measure Infectivity of Filtered Bioaerosols in Mice. *J Appl. Micro.*, In Press 2012.

62. Stone, B.; Heimbuch, B. et al., Design, Construction and Validation of a Nose-Only Inhalation Exposure System to Measure Infectivity of Filtered Bioaerosols in Mice. *J Appl. Micro.*, In Press 2012.

63. Stuart, B. Deposition of Inhaled Aerosols. *Arch. Intern. Med.* 1973, *131*, 60–73.

64. Szretter, K.; Balish, J. et al. *Current Protocols in Microbiology; Unit 15G.1 Influenza: Propagation, Quantification, and Storage*. John Wiley & Sons, Inc., 2005.
65. Tang, J.; Li, Y. Reflection and Reaction—Transmission of Influenza A in Human Beings. *Lancet Infect. Dis*. 2007, *7*, 758.
66. Taubenberger, J., Morens, D. The pathology of influenza virus infections. *Annu. Rev. Pathol.* 2008, *3*, 499–522.
67. Tellier, R. Questioning Aerosol Transmission of Influenza: In Response. *Emerging Infect. Dis.* 2007 a, *13*, 174–175.
68. Tellier, R. Reflection and Reaction- Transmission of Influenza A in Human Beings. *Lancet Infect. Dis*. 2007b, *7*, 759–760.
69. Tellier, R. Review of Aerosol Transmission of Influenza A Virus. *Emerging Infect. Dis.* 2006, *12*, 1657–1662.
70. Treanor, J. Influenza Vaccine—Outmaneuvering Antigenic Shift and Drift. *N. Engl. J. Med.* 2004, *350*, 218–220
71. Twine, S.; Shen, H.; Kelly, J.; Chen, W.; Anders, S.; Conlan, J. Virulence comparison in mice of distinct isolates of type A *Francisella tularensis*. *Microb. Pathog*. 2006, 40, 133-138.
72. van Riel, D.; Munster, V. et al. Human and avian influenza viruses target different cells in the lower respiratory tract of humans and other mammals. *Am. J. Pathol.* 2007, *171*(4), 1215–1223.
73. van Riel, D.; den Bakker, M. et al. Seasonal and Pandemic Human Influenza Viruses Attach Better to Human Upper Respiratory Tract Epithelium than Avian Influenza Viruses. *Am. J. Pathol.* 2010, *176*, 1614–1618.
74. Vlodavets, V.; Dmitriyeva, R. Viability of Respiratory Viruses in the Air. *J. Microbiol., Epidemiol., Immunobiol*. (English translation). 1966, *9*, 30-34.
75. (WHO) World Health Organization Collaborating Centre for Influenza (2009) "CDC protocol of realtime RTPCR for influenza A(H1N1) revision 2 (6 October 2009), " p. 5, http://www.who.int/csr/resources/publications/swineflu/CDCRealtimeRTPCR_SwineH1 Assay-2009_20090430.pdf
76. Wong, B. Inhalation Exposure Systems: Design, Methods, and Operation. Toxicol. Path. 2007, *35*: 3–14.
77. Yang, W.; Elankumaran, S. et al. Concentrations and size distributions of airborne influenza A viruses measured indoors at a health centre, a day-care centre and on aeroplanes. *J. Roy. Soc., Interface.* 2011, *8*(61), 1176–1184.

LIST OF TABLES

LIST OF FIGURES

LIST OF ABBREVIATIONS

ABSL- animal biosafety laboratory

APS- aerodynamic particle sizer

ASHRAE- American Society of Heating, Refrigeration, and Air-conditioning Engineers, Inc.

ATCC- American type culture collection

CATS- controlled aerosol test system

CDC- centers for disease control and prevention

CFU- colony forming unit

CPE- cytopathic effect

DFA- direct fluorescence antibody test

DI- deionized

D_p- presented dose

EMEM- Eagle's minimum essential medium

H&E- hematoxylin and eosin

H1N1- hemagglutinin type 1 and neuraminidase type 1

H5N1- hemagglutinin type 5 and neuraminidase type 1

HEPA- high efficiency particulate air

LPM- liters per minute

LVS- live vaccine strain

MDCK- Madin-Darby canine kidney cells

MID_{50}- median infectious dose

MOI- multiplicity of infection

MPPS- most penetrating particle size

NIAID- national institute of allergy and infectious diseases

NIH- national institutes of health

NOIES- nose only inhalation exposure system

OD- optical density

PASS- power analysis and sample size

PBS- phosphate buffered saline

PFU- plaque-forming unit

PSD- particle size distribution

PSL- polystyrene latex

RH- relative humidity

RNA- ribonucleic acid

RPE- respiratory protection equipment

qRT-PCR- reverse transcription polymerase chain reaction

SMPS- scanning mobility particle sizer

$TCID_{50}$-median tissue culture infectious dose

UNMC- University of Nebraska Medical Center

VSF- viable spray factor

Appendix A. **Power Analysis for Using Mice to Detect Difference in Infectivity**

A power analysis was performed at UNMC to determine the number of mice (n) needed per group to attain a statistically reliable discrimination of difference in infectivity between two groups of animals in a filtration penetration study using the following general design:

The MID_{50} was derived using an unexposed control group and evaluating six challenge concentrations, nominally centered around the MID_{50}, delivered to groups of 5 mice per concentration. Rates of infection in pairs of groups of mice—treated and control—were compared. The MID_{50} is the dose that causes a 50% rate of infection in the treated group. The power of the experimental design to distinguish a difference in infection rate between the two groups is calculated in Table A1 for a range of per cent differences and group sizes. PASS software was used to calculate the sample sizes needed to detect differences between the groups under the following conditions: Two-sided test; Significance level (alpha) = 0.05; n = number in each group

Table A. Power to Detect Differences between Treated and Control Groups of Different ns

Proportion Infected		Difference Detected	n per	Power
Control	Treated	(Treated - Control)	group	(%)
0.40	0.05	-0.35	10	42.65
0.40	0.05	-0.35	12	54.95
0.40	0.05	-0.35	15	69.53
0.45	0.05	-0.40	10	52.98
0.45	0.05	-0.40	12	65.69
0.45	0.05	-0.40	15	79.38
0.50	0.05	-0.45	10	62.80
0.50	0.05	-0.45	12	75.18
0.50	**0.05**	**-0.45**	**15**	**86.97**
0.55	0.05	-0.50	10	71.75
0.55	0.05	-0.50	12	83.11
0.55	0.05	-0.50	15	92.35
0.60	**0.05**	**-0.55**	**10**	**79.58**
0.60	0.05	-0.55	12	89.32
0.60	0.05	-0.55	15	95.85
0.55	0.10	-0.45	10	56.60
0.55	0.10	-0.45	12	70.10
0.55	0.10	-0.45	15	81.03
0.60	0.10	-0.50	10	65.90
0.60	0.10	-0.50	12	79.07
0.60	0.10	-0.50	15	87.67

A sample size of 15 mice per group (30 total), provides 87% power to detect a 45% difference between the groups. Ten mice per group gives 80% power to detect a 55% difference between the groups. As cost was a factor, the statistician extrapolated that a sample size of 5 per group would provide adequate power to discriminate a difference of 50%.

Appendix B. Intranasal Inoculation of Three Mouse Strains

Table B. Weight change of three strains of mice before and after intranasal inoculation with one of two dilutions of H1N1.

Mouse	Viral Dose (TCID$_{50}$ Units)	Day 1–7 Weight Change (g)	Viral Dose (TCID$_{50}$ Units)	Day 1–7 Weight Change (g)	Viral Dose (TCID$_{50}$ Units)	Day 1–7 Weight Change (g)
CD57BL[a]						
1		-6.0		-5.4		-0.4
2		-5.3		-5.7		+0.2
3	1.4 x 10^6	-5.3	1.4 x 10^5	-4.9	0 (control)	+0.3
4		-5.1		-5.3		
5		-5.3		-5.6		
Avg. Wt. Change (g)		-5.4		-5.4		0.0
Standard Deviation		0.4		0.3		0.3
Avg. % Wt. Change[b]		-28.2		-28.0		-0.1
Standard Deviation		1.3		1.7		1.9
BALB/c[c]						
1		-4.5		-3.6		-0.3
2		-4.5		-3.3		-0.2
3	1.4 x 10^6	-4.6	1.4 x 10^5	-3.7	0 (control)	-0.2
4		-4.9		-3.7		+0.3
5		-5.1		-2.9		
Avg. Wt. Change (g)		-4.7		-3.4		-0.1
Standard Deviation		0.3		0.3		0.3
Avg. % Wt. Change		-26.3		-19.0		-0.5
Standard Deviation		2.2		1.6		1.6
CD-1[d]						
1		-7.6		-6.4		-0.2
2		-5.4		-5.9		0.0
3	1.4 x 10^6	-5.8	1.4 x 10^5	-5.7	0 (control)	+0.1
4		-7.8		-5.8		
5		*		-5.4		
Avg. Wt. Change (g)		-6.6		-5.8		0.0
Standard Deviation		1.2		0.3		0.2
Avg. % Wt. Change		-26.1		-23.6		-0.2
Standard Deviation		3.8		0.9		0.6

"-" Indicates weight loss, "+" Indicates weight gain, "*" Indicates deceased mouse, not used in calculations. [a] $19.20 each. [b] [(Initial-final)/ initial] x 100 [c] $18.74 each. [d] $4.80 each

Appendix C. Initial Aerosol Exposure Experiments

Table C. Weight Changes of Mice after Inhalational Exposure to Two Challenge Levels of Aerosolized H1N1 Virus for Different Lengths of Time at 25 °C, 54–59% Relative Humidity

Mouse	Exposure Time (mins)	Day 1-7 Weight Change (g)	
		1.58×10^6 TCID$_{50}$/mL	1.58×10^5 TCID$_{50}$/mL
1	2	-0.4	-0.2
2		+1.0	+1.1
3		-1.9	+1.5
Avg. Wt. Change (g)		-0.4	+0.8
Standard Deviation		1.5	0.9
Avg. % Wt. Change		-2.1	+2.8
Standard Deviation		6.7	3.4
1	6	-2.5	+0.5
2		*	+1.3
3		-2.2	+0.3
Avg. Wt. Change (g)		-2.4	+0.7
Standard Deviation		0.2	0.5
Avg. % Wt. Change		11.5	+2.9
Standard Deviation		1.2	2.1
1	20	-3.9	+2.8
2		-3.5	-0.4
3		-4.5	-1.0
Avg. Wt. Change (g)		-4.0	-0.5
Standard Deviation		0.5	2.0
Avg. % Wt. Change		-21.0	+1.8
Standard Deviation		3.6	7.9
1	60	-3.4	-2.6
2		-5.1	-1.2
3		-1.3	-0.8
Avg. Wt. Change (g)		-3.2	-1.5
Standard Deviation		1.9	1.0
Avg. % Wt. Change		-17.9	-6.9
Standard Deviation		11.4	4.2
1	0	*	+1.7
2		+1.9	+0.5
3		+1.3	+1.8
Avg. Wt. Change (g)		+1.6	+1.3
Standard Deviation		0.5	0.7
Avg. % Wt. Change		+6.5	+5.1
Standard Deviation		1.9	2.7

"-" Indicates weight loss, "+" Indicates weight gain, "*" Indicates deceased mouse, not used in calculations.

Infected mice were characterized by marked weight loss then later confirmed by PCR and virus viability assays using CPE. Lung homogenates were harvested in BD Universal Virus Transport media, separated into three aliquots and frozen at -80 ˚C.

Figure C. MDCK cell plates of mouse lung homogenates after crystal violet dye.

Exposure Time = 0 mins   2 mins   6 mins

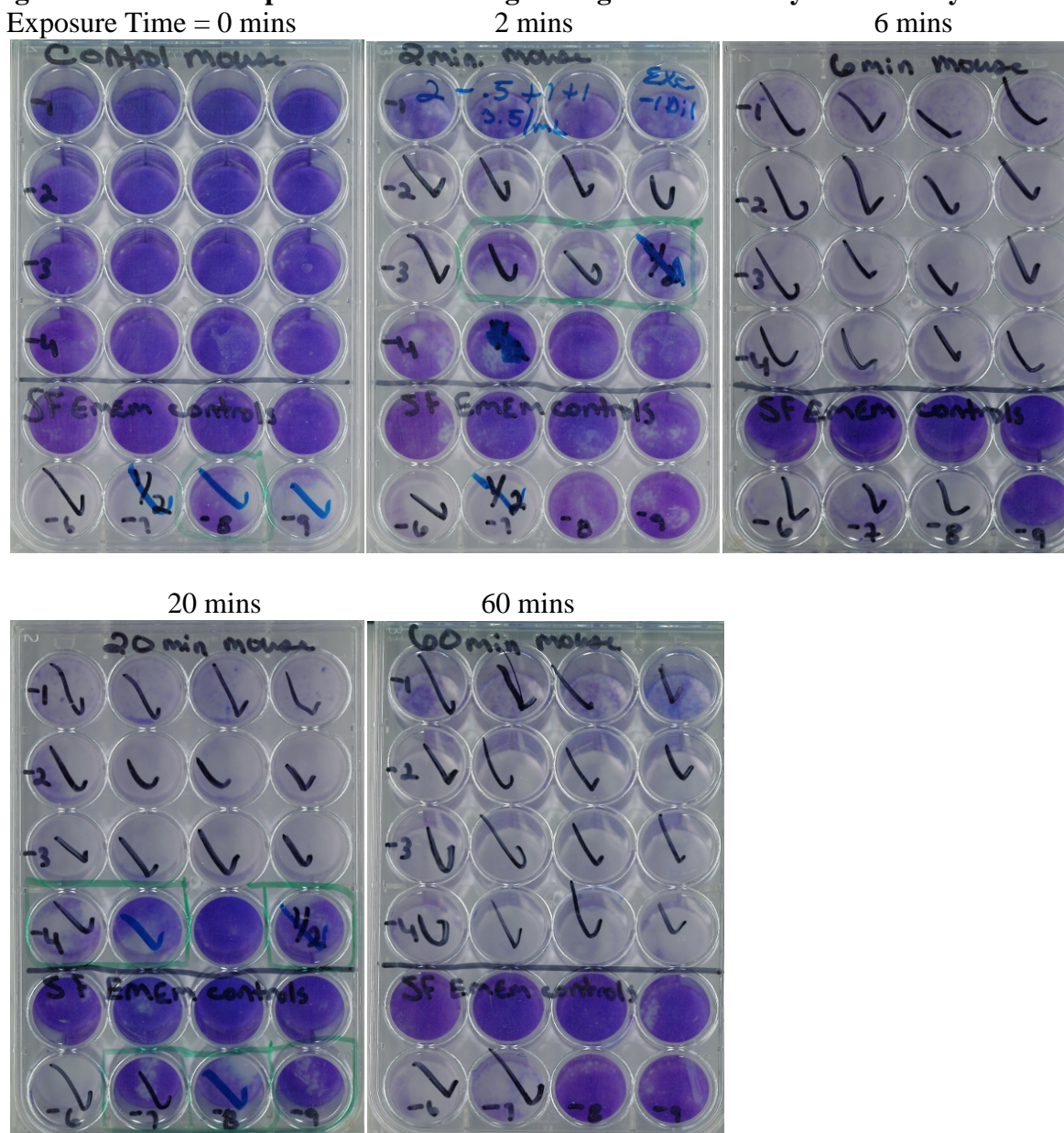20 mins   60 mins

Appendix D. Final Aerosol Exposure Experiment

Table D. Weight Changes of Mice after Inhalational Exposure to Aerosolized H1N1 Virus[a] for Different Lengths of Time at 25 °C, Relative Humidity Rising from 26–69%

Exposure Time (mins)	Day 1-7 Weight Change (g)						
	3	6	9	12	18	18[b]	18[c]
Mouse 1	+0.2	+2.0	+1.1	+3.1	+1.6	+2.2	+1.2
Mouse 2	+1.6	+4.2	*	+0.4	+1.4	*	+1.1
Mouse 3	+1.7	+2.0	+1.3	+1.4	+1.0	+1.6	+1.7
Mouse 4	-0.1	+0.2	+0.9	+0.7	+1.4	+0.5	+1.6
Mouse 5	+2.0	+1.9	-0.4	+3.0	+0.3	+2.6	+2.0
Avg. Wt. Change (g)	+1.1	+2.1	+0.7	+1.7	+1.2	+1.7	+1.5
Standard Deviation	1.0	1.4	0.8	1.3	0.5	0.6	0.4
Avg. % Wt. Change	+4.3	+8.6	+3.2	+6.7	+4.8	+7.2	+6.1
Standard Deviation	3.8	6.1	3.2	5.0	2.2	4.1	1.6

"-" Indicates weight loss; "+" Indicates weight gain; "*" Indicates mouse died of unrelated causes, did not use to calculate data; [a] Titer in Collison 4.74×10^7 $TCID_{50}$/mL; [b] sterile medium control; [c] sterile allantoic fluid control

Figure D. Typical 96-well Plates of MDCK Cells Exposed to Mouse Lung Homogenates then Crystal Violet Dye. Image Shows Group 1 Exposed for Seven Time Points: 0 mins (NV), 0 mins (CM), 3 mins, 6 mins, 9 mins, 12 mins, and 18 mins. NV = allantoic fluid with no virus present, CM = control mouse exposed to sterile aerosols.
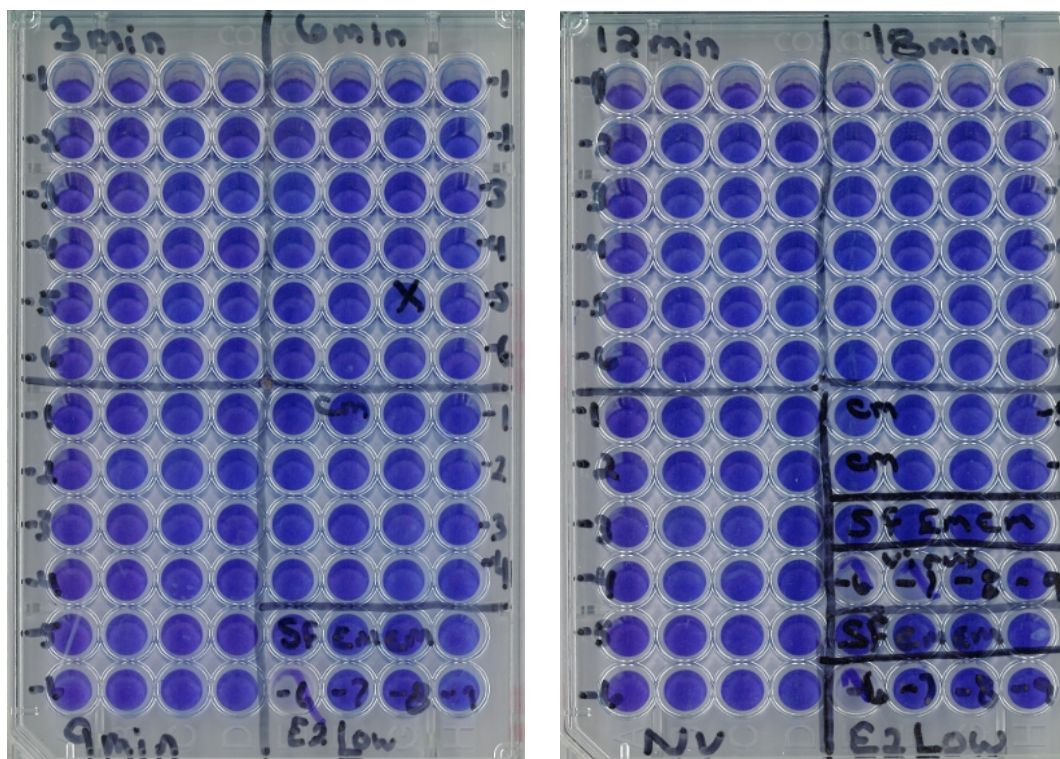
Appendix E. Presented Dose of Influenza Aerosol and PCR, Fluorescent Assay and Cytopathic Effect Results for All Three Aerosol Exposure Concentrations

Table E. Presented Dose of Influenza Aerosol and PCR, Fluorescent Assay and Cytopathic Effect Results

Titer[a] (TCID$_{50}$/mL)	n	Exposure Time (min)	D_p (TCID$_{50}$)	Weight Change (% ± SD)	PCR Ct	DFA	CPE
1/30 * 4.74x10^7= 1.58x10^6	5	2	119	-1.7 ± 6.4	Pos (23)[b]	Pos[b]	Pos[b]
		6	356	-40.2 ± 51.8[*]	Pos (18)[b]	Pos[b]	Pos[b]
		20	1190	-17.3 ± 2.4	Pos (16)[b]	Pos[b]	Pos[b]
		60	3560	-14.6 ± 8.4	Pos (17)[b]	Pos[b]	Pos[b]
	3	Control	0	+6.9 ± 2.1	Neg (37)[b]	Neg[b]	Neg[b]
1/300 * 4.74x10^7= 1.58x10^5	3	2	11.9	+2.8 ± 3.4	Pos (23)[b]	Pos[b]	Pos[b]
		6	35.6	+2.9 ± 2.1	Pos (18)[b]	Pos[b]	Pos[b]
		20	119	+1.8 ± 7.9	Pos (16)[b]	Pos[b]	Pos[b]
		60	356	-6.9 ± 4.2	Pos (17)[b]	Pos[b]	Pos[b]
		Control	0	+5.1 ± 2.7	Neg (37)[b]	Neg[b]	Neg[b]
1/1000 * 4.74x10^7 = 4.74x10^4	5	3	5.34	+4.3 ± 3.8	5 Neg	5 Neg	5 Neg
		6	10.7	+8.6 ± 6.1	1 Pos 4 Neg	1 Pos 4 Neg	1 Pos 4 Neg
		9	16.0[*]	+3.2 ± 3.2	1 Pos 1 Neg 2 Ind	1 Pos 3 Neg	1 Pos 3 Neg
		12	21.4	+6.7 ± 5.0	1 Pos 3 Neg 1 Ind	1 Pos 4 Neg	1 Pos 4 Neg
		18	32.1	+4.8 ± 2.2	1 Pos 1 Neg 3 Ind	2 Pos 3 Neg	2 Pos 3 Neg
		18[c]	0	+7.2 ± 4.1	5 Neg	5 Neg	5 Neg
		18[d*]		+6.1 ± 1.6	4 Neg	4 Neg	4 Neg

[a] of fluid delivered into the Collison nebulizer; [b] measured for a single mouse rom the group of 5; [c] sterile allantoic fluid control; [d] sterile medium control. Parameters: Viral titer = 4.74 x 10^7; VSF = 9.00 x 10^{-7}; Resp Rate = 261/min; Tidal Vol = 0.16 mL; [*] mouse died during observation stage due to unrelated cause; Neg = negative; Pos = positive; Ind = indeterminate

Appendix F. Procedure for Inoculation of Embryonated Chicken Eggs
(WHO ANIMAL INFLUENZA MANUAL, 2002)
NOTE: All working steps during this procedure were performed in a class 2 biosafety cabinet.

Materials required
• embryonated chicken eggs, 10 days old
• egg candler
• 70% ethanol
• needle, 22 gauge, 1½ in
• syringe, 1 mL
• egg hole punch
• glue or varnish
• 15-mL tubes and rack
• 10-mL pipettes
• forceps (sterile)

Procedure
I. Candling of eggs [We were unable to see embryo in light, so we proceeded without this step.]
1. Examine eggs with an egg candler and place with blunt end up into egg trays.
2. Discard any eggs that are infertile, have cracks, are underdeveloped, or that appear to have a porous shell.
II. Inoculation of eggs
1. Place eggs with blunt end up into egg trays and label each egg with a specific identification number (3 eggs per specimen).
2. Wipe the tops of the eggs with 70% ethanol and punch a small hole in the shell over the air sac. Three eggs per specimen are usually inoculated.
3. Aspirate 1 mL of processed clinical specimen into a tuberculin syringe with a 22-gauge, 1½-in needle.
4. Holding the egg up to the candler, locate the embryo. Insert the needle into the hole of the egg. Using a short stabbing motion, pierce the amniotic membrane and inoculate 100 μL into the amniotic cavity.
Withdraw the needle about ½ in and inoculate 100 μL of the specimen into the allantoic cavity. Remove the needle.
5. Inoculate the two other eggs in the same manner with the same syringe and needle for a total of three eggs inoculated per specimen.
6. Discard syringe into a proper safety container.
7. Seal the holes punched in the eggs with a drop of glue.
8. Incubate the eggs at 33–34 °C for 2–3 days.
Note: Avian influenza 35 °C or 37 °C (avian viruses also grow well at 35 ℃)
III. Harvesting of inoculated chicken eggs
1. Eggs are chilled at +4 °C overnight or for 4 hrs before harvesting.
2. Label one 15-mL plastic tube for each egg with the specimen number. Clean off the top of each egg with 70% ethanol.
3. With sterile forceps, break the shell over the air sac and push aside the allantoic membrane with the forceps. Using a 10-mL pipette, aspirate the allantoic fluid and place in a labeled plastic tube. Then using a syringe and needle, pierce the amniotic sac and remove as much amniotic fluid as possible. Place harvest in a separate tube, but because of the low volume of amniotic fluid obtained from each egg, it is usually necessary to combine the amniotic fluid from the three eggs inoculated per specimen.
4. Centrifuge harvested fluids at 3000 rpm/5 min to remove blood and cells. [Reported procedure uses a hemagglutination inhibition that we did not perform.]

Appendix G. Procedure for Infection of MDCK Cells with Influenza Virus

This addendum describes the materials used and methods developed for the use of live influenza virus in air filtration studies and subsequent assays.

Materials
• MDCK cell line (ATCC CCL-34)
• Influenza A/PR/8/34 (H1N1) virus was obtained from American Type Culture Collection (Rockville, MD) as frozen stock (ATCC VR-1469)

Buffers and culture media
• Complete growth medium
• Dulbecco's Modified Eagle's Medium (DMEM; HyClone, cat # SH30244.01) supplemented with 10% heat inactivated (45 min at 56 °C) fetal bovine serum (FBS; HyClone, SH30070.03HI) and 1% penicillin/streptomycin (pen-strep, Sigma, cat # P4333)
• Infection medium
• DMEM supplemented with 0.3% bovine serum albumin (BSA; Sigma, cat # A8412) and 1% pen-strep
• Trypan blue dye (Cellgro, Mediatech, Fisher cat# MT-25-900-CI)
• Trypsin–EDTA solution
0.25% trypsin, 2.21 mM EDTA in HBSS (without Ca, Mg, NaHCO3) (Hyclone, cat # SH30042.01)
• Gamma-irradiated trypsin (Worthington, TRLVMF)
• 2X DMEM/BSA Dulbecco's Modified Eagle's Medium supplemented with 0.6%   BSA and pen-strep (2%)

Consumable Stock
• 175-cm2 flasks	• CO_2 tank and regulator
• 24- or 96-well plates	• 37 °C incubator with 5% CO_2
• Haemocytometer	• Water bath
• Haemocytometer cover glass	• -80 °C freezer or liquid N_2 storage tank
• Cryopreservation vials (2 mL)	• 12-channel multipipette
• 50-mL conical tubes	

Procedure for hatching MDCK cells from freezer stock
1. Remove (4) cryogenic vials containing 1 mL stock culture of MDCK cells from -80 ˚C freezer and thaw.
2. Spray each vial with 70% ethanol before opening.
3. Add 9 mL Complete EMEM to (4) T-25 vented tissue culture flasks.
4. Pipette 1 mL of MDCK cells into each T-25 tissue culture flask.
5. Add 1 µL plasmocin (Invivogen ANTMPP) per 10 mL.
6. Add 50 µL fungin (Invivogen ANTFN1) per 10 mL.
7. Incubate the flasks at 37ºC with 5% CO2 until 90% confluency is observed (~4 days).

Procedure for transfer of MDCK cells from T-25 to T-75 flasks
1. Remove the T-25 flasks from the incubator. Rinse the flasks 3x with 5 mL SF EMEM.
2. Add 3mL of trypsin-EDTA, 1X, to each flask. Incubate 20 minutes.
3. If MDCK cells appear to be attached, gently tap flasks on counter to loosen cells and increase turbidity.
4. Pipette 3 mL of complete EMEM down the side of each T-25 flask to remove any loose cells on the flask wall.
5. Combine the cells into 1 flask. Add 300 µL of MDCK cells to a 1.5 mL microcentrifuge tube containing 300 µL trypan blue.
6. Allow 3 minutes for the trypan blue to stain any dead cells.
7. Pipette a small amount of the mixture under the hemacytometer coverslip.
8. Place the hemacytometer under the microscope and count the number of cells in the 4 outer corners. Average the 4 corners to get the number of cells/mm2. Multiply this number by 2 for the 1:2 dilution in trypan blue. Multiply that number by 10 to convert units to cells/mm3. Multiply by 1000 to convert units to cells/cm3 or cells/mL.

Procedure for seeding T-75 flasks with MDCK cells
1. Seed (3) new T-75 vented tissue culture flasks at 5 x 104 cells/mL. Each flask should contain a total volume of 25 mL, therefore, 75 mL total volume will be needed to seed 3 flasks.
2. (Hemacytometer count in cells/mL) (x mL cells) = $(0.5 \times 10^5$ cells/mL) (75 mL)
 x = mL of cells needed to obtain a 5×10^4 concentration
3. Divide x by 3 to give you the amount of MDCK cells needed in each of the T-75 flasks. Subtract that number from 25 mL (total volume per flask) to give you the amount of complete EMEM to add to each T-75 flask.
4. Pipette the MDCK cells and the complete EMEM into the new T-75 flasks. Add 2.5 µL plasmocin (Invivogen ANTMPP) per flask. Add 125 µL fungin (Invivogen ANTFN1) per flask. Incubate the flasks at 37ºC with 5% CO_2.

Procedure to harvest cells from T-75 flasks
For best results, harvest the MDCK cells before they reach 100% confluency

1. Remove the media from each T-75 tissue culture flask and discard into a 4 L Nalgene "BacDown" container.
2. Wash the cells 3 times with 10 mL Serum-free EMEM. Discard each wash.
3. Add 5 mL of Trypsin-EDTA, 1X (Mediatech 25-052-Cl), to each flask. Incubate 20 mins at 37 °C.
4. If MDCK cells appear to be attached, tap flasks on counter to loosen cells and increase turbidity.
5. Pipette 5 mL of Complete EMEM down the side of each flask to remove any loose cells on the flask wall.
6. Repeat the hemacytometer step above and seed 3 new T-75 flasks. Incubate at 37 °C with 5% CO_2.
7. Use the remaining MDCK cells to seed 24- or 96-well plates or to make a freezer stock with 7.5% DMSO. Pipette 1 mL aliquots into 2 mL cryovials and freeze at -80 °C.

8. Repeat every other day using 3 new T-75 flasks each time. Hatch new MDCK cells at the beginning of every month.

Preparation of 24-well plates for H1N1 infection
1. Remove the plates from the incubator and empty the media from the plates into a Nalgene "BacDown" tray.
2. Wash each well containing cells 3x with 500 µL Serum-free EMEM. Empty each wash into the tray.
3. If the virus dilutions are not ready, the wells can be stored with 500 µL SF EMEM at 37 °C with 5% CO_2 until ready.

Titration of virus stocks and samples
1. Make tenfold dilutions of virus in Serum-free EMEM. An allantoic fluid virus stock will often have a titer of about 10^9 $TCID_{50}$/mL, and a tissue culture virus stock will typically have a titer of 10^8 $TCID_{50}$/mL.
2. Prepare dilutions from 10^{-2} to 10^{-10} in 15 mL flip-top tubes, i.e., add 9.90 mL SF EMEM to the 1st tube and 9 mL of Serum-free EMEM to each of the remaining tubes. It is very important to use a new pipette tip between each dilution because influenza will stick to the plastic; If the pipette tips are not changed, the titer will not be accurate.
3. Add 100 µL virus to the first tube containing 9.90 mL of Serum-free EMEM. Vortex the liquid and transfer 1 mL of this dilution to the next tube. Repeat for each dilution.

Inoculation of MDCK cells
1. After the 24-well plates have been rinsed with SF EMEM, add 1 mL of each virus dilution or sample into quadruplicate wells. If the plates were being stored in the incubator with SF EMEM, the SF EMEM should be discarded before inoculating the cells.
2. Set up two sets of control wells: four containing only the SF EMEM (negative controls) and 4 containing influenza virus in a 1:10 serial dilution.
3. Incubate the plates for 1 hour at 37 °C with 5% CO_2. Then add 100 µL of EMEM-1% BSA-trypsin to each well. Incubate at 37 °C with 5% CO_2 for 4 days.

Determination of Titer by CPE
1. Days 2-4, observe CPE under the microscope. The cells should be rounded and many should be lifted from the plate.
2. Discard the supernatant.
3. Stain each of the plate's wells with 400 µL crystal violet–glutaraldehyde; stain for 3 hours (reduced time results in less intense staining).
4. Wash the dye from the plate under running water; collect the rinse for proper disposal.
5. Allow the plates to dry before examining the CPE. The inverse of the dilution at which 50% of the wells show CPE is recorded as the tissue culture infectious dose ($TCID_{50}$). Since this result was obtained by infection of cells with 100uL of the virus dilution, multiply this by 10 to report results as $TCID_{50}$/mL.

Preparation of Crystal Violet Stain
Crystal violet   0.5 g
Gluteraldehyde   75 mL   Deionized Water 675 mL

Analysis of Data

The Spearman–Karber formula was used to determine the concentration of viable virus per mL of extract (L, expressed in units of $\log_{10} TCID_{50}/mL$). Equation 1 was used to determine the total amount of virus recovered from the each sample. (Heimbuch et al., 2009)

Equation 1:

Log titer/mL = lowest fully cleared dilution - 0.5 + 1 + portion of partially cleared well

Titer: $T = 10^{x-0.5+1+y}$ (Spearman–Kärber formula)

where d = log of the dilution (log 10 = 1)

S_p = sum of the proportions

Table G. Ratio and Proportion of Cells Displaying Infection (Clear) at Serially Diluted Levels

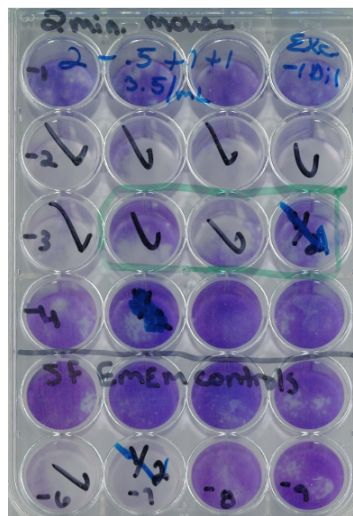| Dilution	Ratio Infected	Proportion Infected
10^{-1}	4/4	1
10^{-2}	4/4	1
10^{-3}	4/4	1
10^{-4}	0/4	0
Neg Control	0/4	0
Pos Control	2/4	0.50

Figure G. 24-well plate post-infection and dye from 2-min mouse on aerosol exposure 1.58×10^5 $TCID_{50}$.

Given the above data for a $TCID_{50}$ assay carried out with 100 µL per well,

Lowest fully cleared dilution (x) = 3
Log titer = x - 0.5 + 1 + y = 3 - 0.5 + 1 + 0.0 = 3.50
Log titer = $10^{3.50}$ = 316 $TCID_{50}$ units (per 100 µL)
Titer = $T = 10^{3.50}$ $TCID_{50}/mL$ = 3.16 x 10^3 $TCID_{50}/mL$